Individual differences in honey bee (*Apis mellifera*) behavior enabled by plasticity in brain gene regulatory networks

Beryl M. Jones[1,*], Vikyath D. Rao[2,3], Tim Gernat[2,4], Tobias Jagla[4], Amy Cash-Ahmed[2], Benjamin E. R. Rubin[5], Troy J. Comi[5], Shounak Bhogale[6], Syed S. Husain[7], Charles Blatti[2], Martin Middendorf[4], Saurabh Sinha[2,6], Sriram Chandrasekaran[7,8,‡], Gene E. Robinson[2,9,10,‡]

[1]Program in Ecology, Evolution, and Conservation Biology, University of Illinois at Urbana–Champaign, Urbana, IL, USA
[2]Carl R. Woese Institute for Genomic Biology, University of Illinois at Urbana–Champaign, Urbana, IL, USA
[3]Department of Physics, University of Illinois at Urbana–Champaign, Urbana, IL, USA
[4]Swarm Intelligence and Complex Systems Group, Department of Computer Science, Leipzig University, Leipzig, Germany
[5]Lewis-Sigler Institute for Integrative Genomics, Princeton University, Princeton, NJ, USA
[6]Center for Biophysics and Quantitative Biology, University of Illinois at Urbana–Champaign, Urbana, IL, USA
[7]Department of Biomedical Engineering, University of Michigan, Ann Arbor, MI, USA
[8]Center for Computational Medicine and Bioinformatics, University of Michigan, Ann Arbor, MI, USA
[9]Neuroscience Program, University of Illinois at Urbana–Champaign, Urbana, IL, USA
[10]Department of Entomology, University of Illinois at Urbana–Champaign, Urbana, IL, USA

*Current address: Department of Ecology and Evolutionary Biology, Princeton University, Princeton, NJ, USA
[‡] Joint corresponding authors, csriram@umich.edu and generobi@illinois.edu

Abstract

Understanding the regulatory architecture of phenotypic variation is a fundamental goal in biology, but connections between gene regulatory network (GRN) activity and individual differences in behavior are poorly understood. We characterized the molecular basis of behavioral plasticity in queenless honey bee colonies, where individuals engage in both reproductive and non-reproductive behaviors. Using high-throughput behavioral tracking, we discovered these colonies contain a continuum of phenotypes, with some individuals specialized for either egg-laying or foraging and "generalists" that perform both. Brain gene expression and chromatin accessibility profiles were correlated with individual behavioral variation, with generalists intermediate in behavior and molecular profiles. Models of brain GRNs constructed for individuals revealed that transcription factor (TF) activity was highly predictive of behavior,

and behavior-associated regulatory regions had more TF motifs. These results provide new insights into the important role played by brain GRN plasticity in the regulation of behavior, with implications for social evolution.

Introduction

Understanding the genomic regulatory architecture of phenotypic plasticity is necessary to achieve comprehensive knowledge of the mechanisms and evolution of complex traits. While a growing body of knowledge exists on specific regulatory mechanisms involved in developmental plasticity, less is known about the regulation of behavioral plasticity. Behavioral plasticity is of special interest and presents unique challenges, as behavioral traits derive from the integrated actions of genetic, transcriptomic, and neuronal networks (Sinha et al., 2020).

Over the past 20 years, a close relationship between behavioral variation and brain gene expression has been documented across a range of organisms and behaviors (e.g., Zayed and Robinson, 2012). Still, the regulatory architecture underlying connections between the genome, brain, environment, and behavior are not well resolved, in part because behavior is itself a complex phenotype with substantial variation between individuals. To fully understand how genomic and transcriptomic variation is transduced into behavioral plasticity, we need both high-dimensional behavioral data at the individual level as well as information on regulatory genomics for those same individuals.

Modification of gene regulatory networks (GRNs) has emerged as an important driver of plasticity during the development and evolution of morphological phenotypes. For example, gains and losses of *cis*-regulatory elements (e.g., binding sites for transcription factors (TFs)) influence species-specific wing melanization patterns in *Heliconius* butterflies and *Drosophila* flies (Prud'homme et al., 2006; Reed et al., 2011; Werner et al., 2010). Pelvic loss in stickleback fish convergently evolved through deletion of a tissue-specific enhancer of the TF *Pitx1* in multiple natural populations (Chan et al., 2010). In other cases, similar morphological novelties arose independently through modification of distinct developmental programs, as observed for beak size variation across clades of finches (Mallarino et al., 2012). Recruitment of genes involved in developmental plasticity in the evolution of novel phenotypes is thought to be facilitated by the fact that TFs and other regulatory genes often have great temporal flexibility, with extensive variation in expression across developmental time (Dufour et al., 2020).

Similar to its role in morphological variation, plasticity in GRNs is theorized to influence behavioral variation, over both organismal and evolutionary time scales (Sinha et al., 2020). Brain gene expression is often responsive to environmental stimuli (Chandrasekaran et al., 2011; Cummings et al., 2008; Mukherjee et al., 2018; Rittschof et al., 2014; Whitfield et al., 2003) and the regulatory activity of many TFs is context-specific with respect to behavioral state (Chandrasekaran et al., 2011; Hamilton et al., 2019). These results demonstrate that GRNs are plastic not only across developmental timescales but also influence real-time behavioral variation. Still, the link between changes in GRNs and behavioral plasticity is weaker than for developmental plasticity (Sinha et al., 2020), and to our knowledge, no empirical studies have linked brain GRN plasticity to individual differences in behavior.

Eusocial insects are ideal for studying how GRN activity influences both developmental and behavioral plasticity at the individual scale. Eusociality is characterized by a reproductive division of labor between queen and worker castes, representing a developmentally plastic polyphenism well-studied in many species (e.g., Holldobler and Wilson, 1990; Michener, 1974; O'Donnell, 1998; Wheeler, 1986). Queens are specialized for reproductive functions, including mating and egg-laying, and in species with complex eusociality, have levels of fecundity orders of magnitude greater than their solitary ancestors. Workers, on the other hand, typically do not perform reproductive behaviors and in many cases are sterile or unable to mate, instead performing many different non-reproductive behaviors in a colony that are essential for colony growth and development. Species with complex eusociality also often show additional within-caste behavioral plasticity, with individuals specializing on specific subsets of tasks based on differences in worker age, morphology, or genetic predisposition. The extensive behavioral plasticity observed in colonies of eusocial species may be linked to ancestral developmental plasticity (Kapheim et al., 2020), highlighting the interconnectedness of gene regulation in both developmental and behavioral phenotypes relevant for social behavior (Sinha et al., 2020).

We studied the relationship between brain GRN activity and behavioral plasticity at the individual scale. We focused on a recently discovered, surprising form of behavioral plasticity among worker honey bees. Honey bee workers do not mate, but they possess functional ovaries and can produce viable haploid eggs. Laying workers (LW) are rare in queenright colonies (Ratnieks, 1993; Visscher, 1996) but frequent in situations of permanent queenlessness, when colonies lose their queen and then fail to rear a replacement queen. In these cases, up to 50% of

workers may activate their ovaries (Sakagami, 1954) and some of these workers lay eggs, producing thousands of drones prior to colony death (Page Jr and Erickson Jr, 1988). Recently, it was discovered that some LWs engage in both reproductive and non-reproductive behaviors (Naeger et al., 2013), a level of behavioral plasticity not previously described in honey bee workers. Studying honey bee workers in LW colonies enables investigation of the molecular architecture of behavioral variation typically only seen when comparing queens and workers, without the confounds of caste-specific developmental and physiological differences.

Recent advances in machine learning and automatic behavioral tracking have enabled the study of individual behavior for thousands of members within social insect colonies (Crall et al., 2015; Gernat et al., 2018; Greenwald et al., 2015; Mersch et al., 2013; Wario et al., 2015). We used automatic behavioral tracking, genomics, and the extensive behavioral plasticity present in honey bee colonies with LW to test the hypothesis that individual differences in behavior are associated with changes in the activity of brain GRNs, i.e., changes in the expression of TFs and their target genes. Our results provide key insights into the mechanisms underlying the regulation of individual differences in behavior by brain GRNs.

Results

Extensive variation in behavior across laying workers

To define the behavior of individual bees, we deployed a high-resolution, automatic behavior monitoring system on six LW colonies in which each bee (n=800 per colony) was individually barcoded, similar to Gernat et al. (2018). Our extension of this system identifies the location and heading direction of each individual once per second, and uses convolutional neural networks and machine learning to detect behaviors. For each individual across seven days of tracking (when bees were 15-21 days old), egg-laying events and foraging trips were detected from images of the hive interior and entrance (Fig. 1A). A total of 115,281 egg-laying events and 96,086 foraging trips were predicted for the six colonies (File S1).

Colonies exhibited considerable variation in the proportion of bees engaged in egg-laying and/or foraging. With the exception of colony F, more workers were identified as layers than foragers (Fig. 1B). Across all colonies, a high proportion of bees were observed laying eggs (54% with at least two egg-laying events on at least one day) or foraging (28% with at least two foraging trips on at least one day) during the recording period, while 10.8% of bees performed

both egg-laying and foraging on the same day at least once during the seven days of tracking. A small number of these "generalist" bees (1.3%; 45 individuals) were exceptional in their consistent high performance of both measured behaviors, with a minimum of two egg-laying events and two foraging trips on the same day, across at least three days. Three-day ethograms of an egg-layer, generalist, and forager are shown in Fig. 1C. Ovary dissection of a subset of individuals revealed that 100% of specialized egg-layers and generalists had active ovaries (ovary scores of 3-5; Hess 1942), compared with only 54% of the specialized foragers (Fig. 1D, File S2). Of the foragers with activated ovaries, 13/14 had 5 or fewer predicted egg-laying events, compared with generalists and layers, which laid an average of 206 eggs (range: 64-774).

The daily and lifetime behavior of each bee was summarized using two behavioral scores: the "specialist" score, which describes how specialized an individual was on either egg-laying or foraging, and the "generalist" score, which describes how much an individual performed both egg-laying and foraging. Scores were derived from daily normalized ranks within colonies to allow comparison across days and colonies with differing overall activity levels; bees that performed neither egg-laying nor foraging across the experiment have both specialist and generalist scores of 0. Scores were mapped onto a two-dimensional color space for visualization of behavior over time (Fig. 2, File S1).

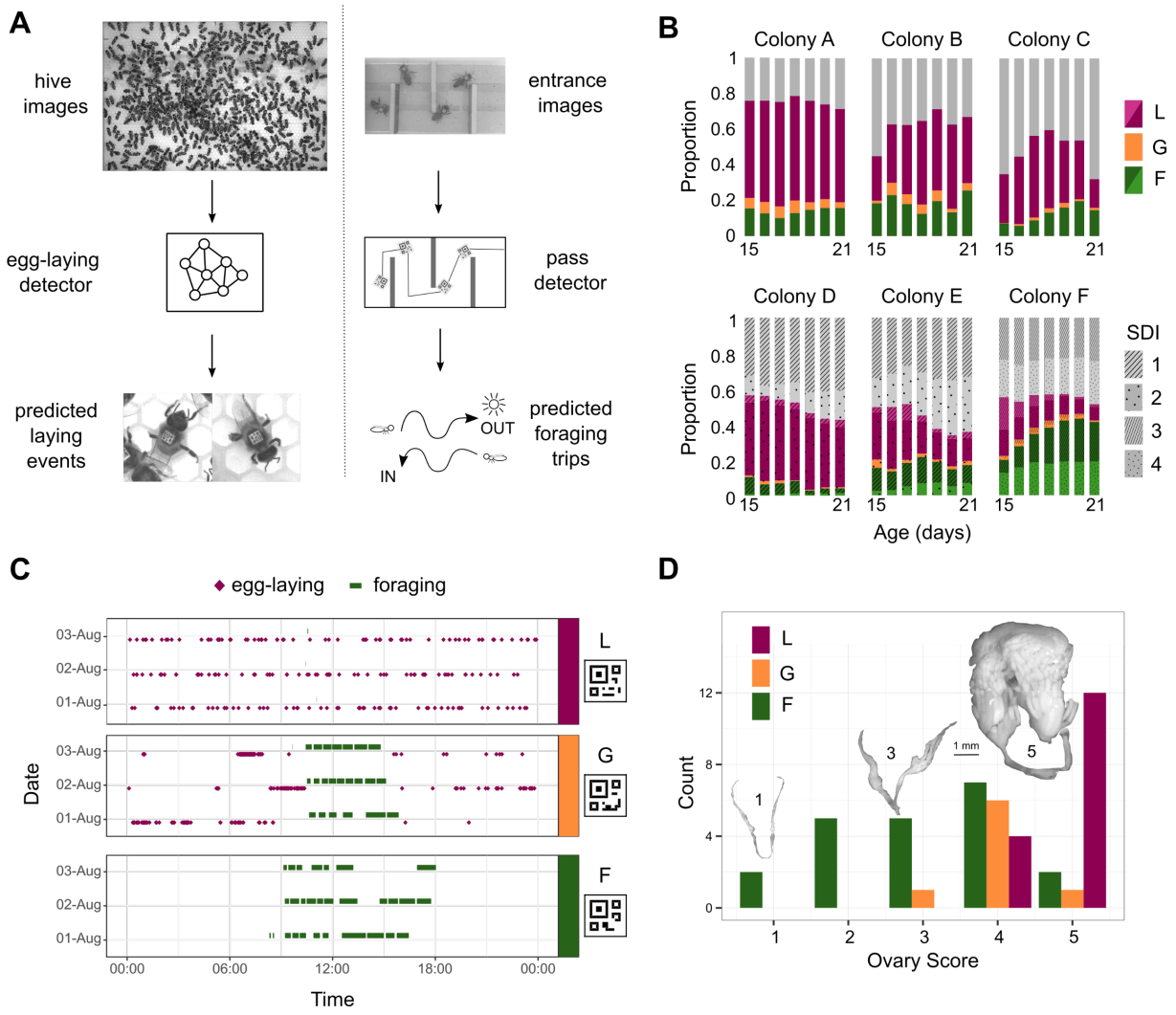

Figure 1. (A) Automatic behavior monitoring was performed inside the hive and at the hive entrance to predict egg-laying and foraging events in six colonies (N=800 bees per colony at the start of each trial). Hive images were captured 1/s for 24 h/day, and entrance images 2/s for 12 h/day beginning when adult bees were 15 days old. **(B)** Proportion of bees alive each day categorized as layers (purple), foragers (green), generalists (orange), or others (gray). For colonies A-C, individuals were from single source colonies headed by a naturally mated queen. For colonies D-F, individuals from two source colonies headed by queens each inseminated by semen from a single different drone (single drone inseminated, SDI) were mixed. Different source colonies are indicated by pattern and hue. **(C)** Ethograms for three individuals selected for sequencing (bCodes shown below group labels) across three days of tracking. **(D)** Distribution of ovary scores for individuals selected for sequencing. Insets are images from bees with ovary scores of 1, 3, and 5. L: layer, G: generalist, F: forager.

151

Influence of worker source colony on behavior

To study the influence of source colony (including genetics and development) on behavior, experimental colonies were assembled with workers from different source colonies headed by unrelated queens. Bees in colonies A-C were derived from colonies with naturally mated queens. Queens of *Apis mellifera* mate multiply with up to ~20 males and produce workers with a mix of paternal genotypes (Adams et al., 1977; Estoup et al., 1994; Lobo and Kerr, 1993); workers derived from these colonies were therefore assumed to be a mix of many patrilines. In contrast, experimental colonies D-F were assembled of workers obtained from two different source colonies, each of which was headed by a queen artificially inseminated with the semen of a single different drone (SDI). Workers within each SDI source colony are highly genetically related compared with workers from a naturally mated queen colony (average relatedness = 0.75 due to haplodiploidy).

Using SDI colonies allowed us to more easily explore whether the genetic and environmental differences between source colonies would lead to segregation of reproductive and non-reproductive behavior when mixed into the same (queenless) environment. In both colonies D and E, which were replicates of the same two SDI queens' offspring, the behavior of workers differed considerably by source: one source colony (SDI 1) comprised the majority of foragers, while the other (SDI 2) contained the majority of egg-layers (Fig. 2). In colony F the two SDI source colony progeny contributed more equally to foraging, while the most specialized egg-laying bees were predominantly from just one source colony (Fig. 2, SDIs 3 and 4). However, even in colonies where SDI source was clearly influential, specialized foragers and layers were identified from both sources, indicating that colony genetics and development are not the only contributors to individual variation in the likelihood of performing these behaviors. Similar patterns of specialization were observed in colonies A-C and D-F (Fig. 2), indicating that they were not an artifact of decreased intracolonial genetic diversity.

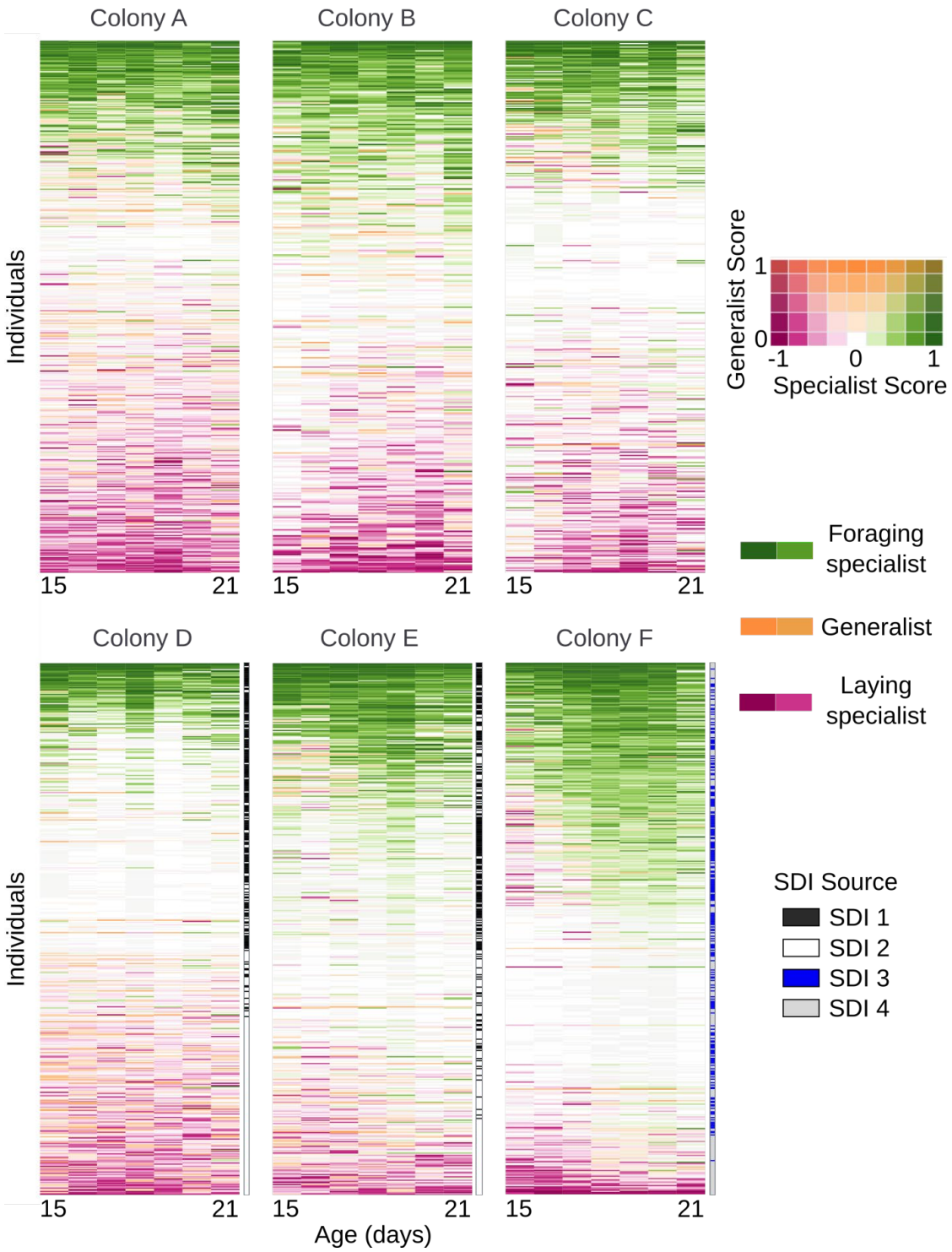

Figure 2. Daily behaviors of individual bees (rows) across time in each colony. Colored rectangles indicate specialist and generalist scores represented in 2D color space as shown in legend. Individuals are sorted by median lifetime specialist score. Single-drone inseminated (SDI) queen source is shown to the right of each row for colonies D-F, where workers were known offspring of two SDI queens per colony. In colonies A-C workers were offspring of naturally mated queens.

178 *Specialized behavioral groups are highly transcriptionally and epigenetically distinct*

179 A subset of highly specialized foragers, egg-layers, and generalist individuals were
180 selected from two experimental colonies (from only one source SDI each) for brain gene
181 expression and chromatin accessibility profiling (Fig. 3A). Principal component analysis (PCA)
182 on behavioral data for these individuals shows these three groups are behaviorally distinct, with
183 generalists intermediate and more variable than forager and layer groups (Fig. 3B).

184 Consistent with strong behavioral differentiation, foragers and layers exhibited
185 widespread differences in brain gene expression, with differential expression of nearly half
186 (46%) of all genes expressed in the brain (Fig. 3C, File S3). Differences in brain gene expression
187 were much stronger between foragers and layers (4506 differentially expressed genes, DEGs)
188 than for generalists relative to the two specialist groups (648 generalist vs. layer and 374
189 generalist vs. forager DEGs). Generalists shared transcriptional profiles of both foragers and
190 layers, with nearly all genes differentially expressed between generalists and either specialized
191 group also present on the forager vs. layer DEG list (Fig. 3C).

192 Forager vs. layer DEGs were enriched for cytoplasmic translation and transport gene
193 ontology (GO) biological processes, along with many metabolic and biosynthetic processes (File
194 S3). All enriched GO terms but one (114 of 115) were for genes more highly expressed in
195 foragers relative to layers (forager-biased genes). The only GO term enriched in layer-biased
196 genes relative to foragers, cytoplasmic translation, was also the only enriched GO term for genes
197 overexpressed in generalists relative to foragers. Similarly, GO terms enriched in generalist-
198 biased genes (relative to layers) included many of the transport terms enriched among forager-
199 biased genes (File S3).

200 In addition to differences in brain gene expression, layers and foragers showed
201 differences in accessible chromatin in the brain based on the Assay for Transposase-Accessible
202 Chromatin using sequencing (ATAC-seq; Buenrostro et al., 2013). 1794 differentially accessible
203 peaks (DAPs) were identified between foragers and layers, proximal to 1207 genes (Fig. 3D, File
204 S4). Forager-biased DEGs and genes proximal to forager-biased DAPs overlapped significantly,
205 1.2x more than expected by chance ($p=0.01$ for hypergeometric test of overlap). Genes proximal
206 to peaks of accessible chromatin (regardless of differential status) were on average more highly
207 expressed than genes without proximal peaks ($p<0.0001$, Kolmogorov-Smirnov test), supporting
208 a signal of transcriptional activation near ATAC-seq peaks (Fig. S1). No DAPs were identified

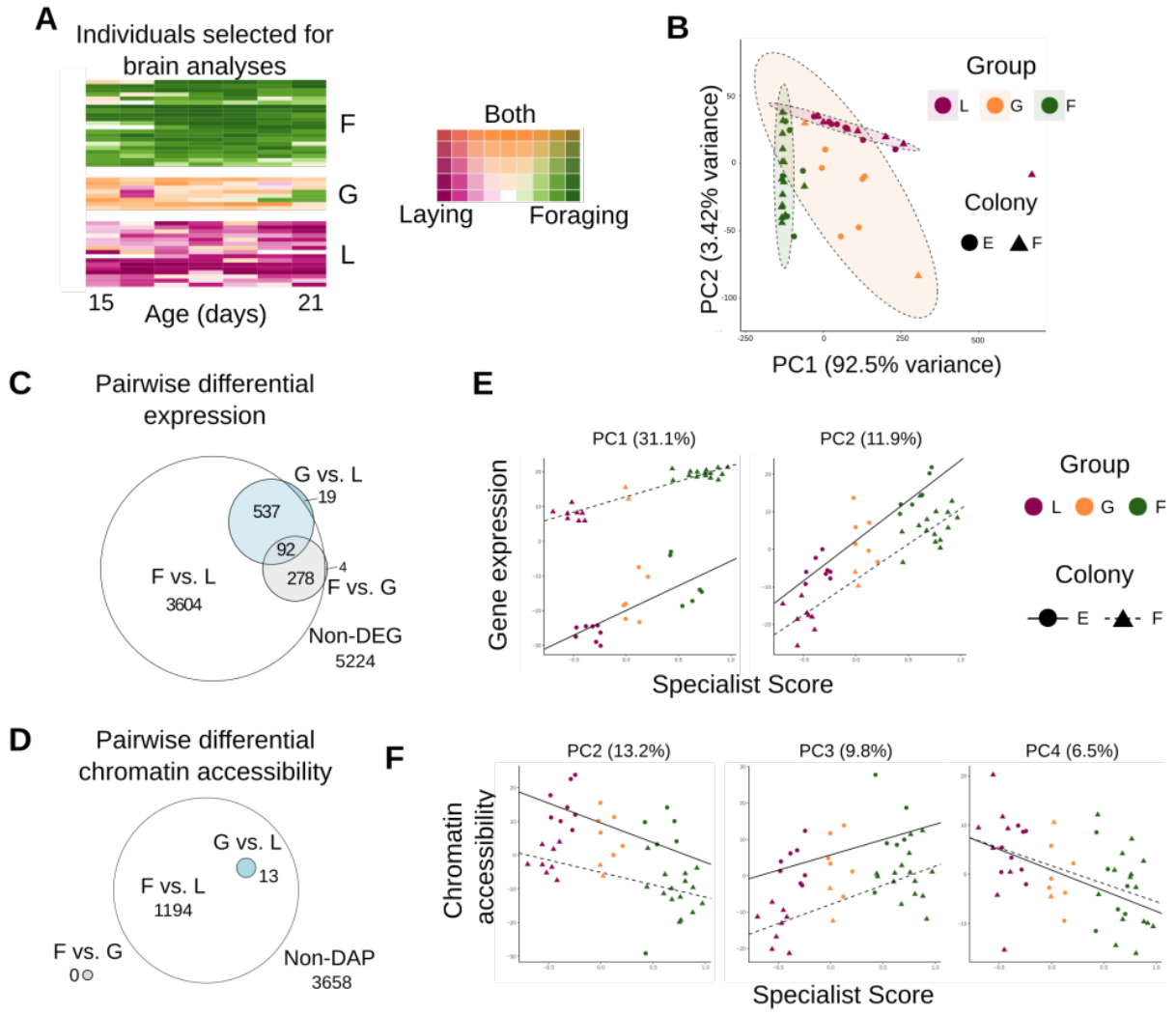

Figure 3. (A) Daily rank-normalized behavior of individuals (rows) selected for brain RNAseq and ATACseq analysis converted to 2D colorspace from specialist and generalist scores. **(B)** Principal Component Analysis (PCA) of behavioral variation for individuals chosen for brain RNAseq and ATACseq analysis. Metrics included number of eggs laid, number of foraging events, proportion of foraging trips with evidence of nectar collection, proportion of trips with evidence of pollen collection, and proportion of trips with evidence of both nectar and pollen collection. **(C)** Euler diagram for overlaps of pairwise differentially expressed genes (DEGs) between behavioral groups. Note that one gene was overlapping between F vs. G and G vs. L (but not F vs. L) and is not represented in the diagram due to graphical constraints. **(D)** Euler diagram for overlaps of genes proximal to pairwise differentially accessible chromatin peaks (DAPs) between behavioral groups. **(E)** PCs from PCA of brain transcriptomic profiles regressed against specialist score (PC1: R^2=0.947, p<0.0001; PC2: R^2=0.838, p<0.001). **(F)** PCs from PCA of brain chromatin accessibility regressed against specialist score (PC2: R^2=0.584, p<0.001; PC3: R^2=0.543, p<0.0001; PC4: R^2=0.187, p<0.0045; PC1: p>0.05). L: layer, G: generalist, F: forager.

210 for foragers relative to generalists, and there were only 16 DAPs (assigned to 13 genes) for
211 generalists relative to layers (Fig. 3D). These 13 genes also had DAPs for foragers relative to
212 layers (Fig. 3D). DAPs between foragers and layers were enriched for 148 GO terms, including
213 developmental processes, morphogenesis, and metabolism (File S4). Similar to differentially
214 expressed genes, GO enrichment signal came from those DAPs with a bias in foragers (i.e., more
215 accessible in foragers relative to layers); no significantly enriched GO terms were identified from
216 layer-biased peaks, despite 44% of differential peaks being more accessible in layers compared
217 to foragers.
218
219 *Brain gene expression and chromatin accessibility are correlated with behavioral variation*
220 Our high-resolution behavioral data allowed us to test whether molecular and behavioral
221 variation were connected not only at the group level, but for individuals as well. Using PCA, we
222 found that degree of individual behavioral specialization was significantly correlated with
223 measures of both brain gene expression and chromatin accessibility (Fig. 3E-F). Among PCs for
224 gene expression, PCs 1 and 2, which explained 31.1% and 11.9% of the total variance in gene
225 expression, respectively, were significantly correlated with individual behavioral specialist score
226 (Fig. 3E). Generalists showed intermediate values of these PCs, consistent with an intermediate
227 brain transcriptomic profile. Genes with extreme PC loading values (upper and lower 5% of
228 loadings) for PC1 were enriched for transmembrane and ion transport, functions related to
229 aerobic and cellular respiration, and energy transport (File S5). PC2 extreme loading genes were
230 enriched for processes relating to detection of light, phototransduction, and sensory perception
231 (File S5). Extreme loadings for both PC1 and PC2 overlapped significantly with DEGs in the
232 pairwise comparison of layers and foragers (PC1: RF=1.2, p=1.39e-06, PC2: RF=1.7, p=8.39e-
233 91).
234 Similarly, PCA of chromatin accessibility data revealed PCs that were correlated with
235 behavioral variation. Accessibility PCs 2, 3, and 4 were all significantly correlated with the
236 individual behavioral specialist score (Fig. 3F). Genes with extreme PC loading values for each
237 correlated PC showed enrichment for multiple GO terms, including biological processes related
238 to cell-cell adhesion, locomotion, axon guidance, neuron projection guidance, and synapse
239 organization (File S6). Many GO terms (11 of 37) were enriched for extreme loading genes of
240 both PCs 2 and 3, while synapse organization was the only enriched term for loadings of PC4.

241

242 *GRN activity links molecular and behavioral phenotypes*

243 To test the role of transcription factor (TF) and gene regulatory plasticity in the regulation
244 of LW behavioral phenotypes, we conducted TF motif analyses and brain GRN reconstruction,
245 individualized for each bee.

246 TF motifs were strongly enriched in peaks of differential accessibility or in the regulatory
247 regions of DEGs between specialized layers and foragers. 77 out of 223 motifs (functionally
248 validated in *Drosophila melanogaster*, Zhu et al., 2011) were enriched in layer vs. forager DAPs
249 (q-val<0.01, File S7), and 14 motifs were specifically enriched in the regulatory regions of
250 forager-upregulated DEGs (q-val<0.2, File S7). Nine motifs were common to both sets (Fig. 4),
251 including binding sites for TFs involved in regulating nervous system development (hairy, side,
252 sr, and klu), transcription (max/mnt), juvenile hormone (JH) signaling (tai and tai/met),
253 chromatin modification (trl), and circadian rhythms (cwo). These motifs were centrally enriched
254 within DAPs (Fig. 4A), and showed two peaks of elevated binding probability in the promoter
255 regions of forager-biased DEGs, one ~3kb upstream of transcriptional start sites (TSSs) and a
256 second overlapping TSSs (Fig. 4B). By contrast, only two TF motifs were significantly enriched
257 in the regulatory regions of specialist vs. generalist DEGs (mad and ken, File S7), and no motifs
258 were enriched within DAPs between generalists and either specialist group (File S7), likely due
259 in part to the small number of DAPs distinguishing generalists and specialists (Fig. 3D). Many of
260 the motifs enriched within DAPs or DEG promoters are binding sites for TFs that were
261 themselves differentially expressed, including cwo, tai/met, side, h, and sr (File S3).

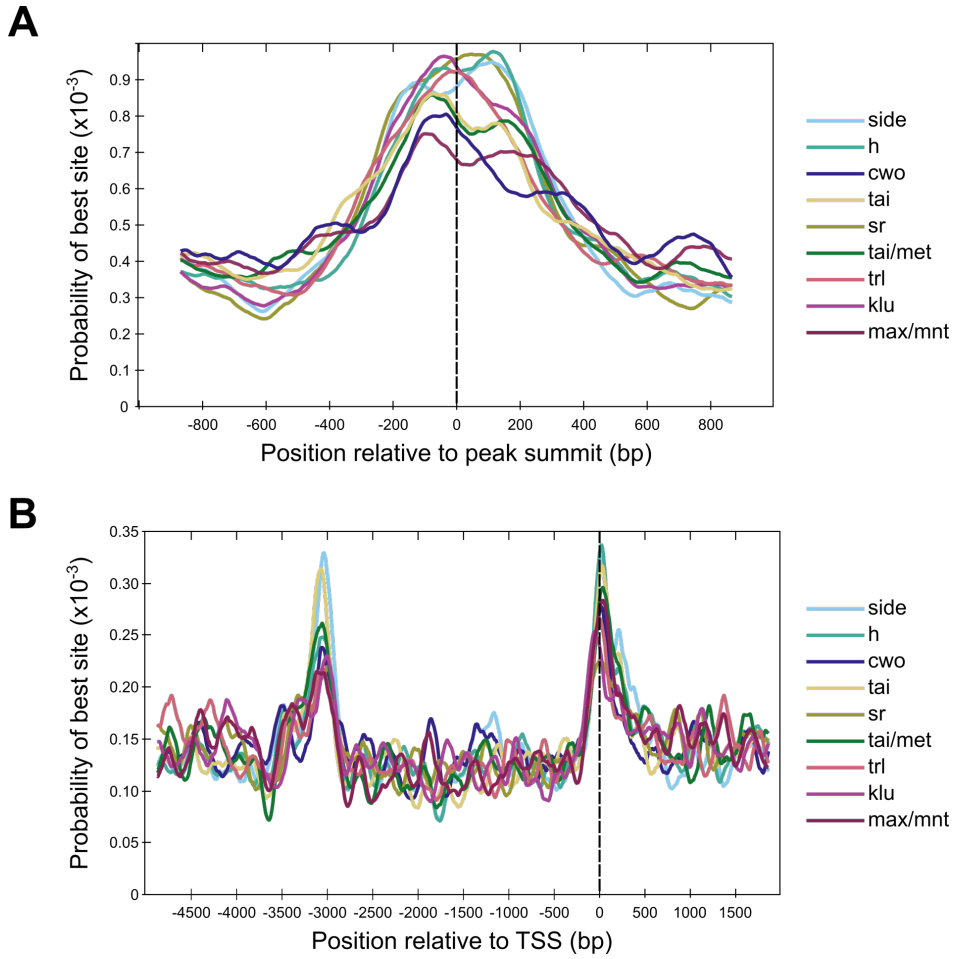

Figure 4. Shared motifs enriched within DAPs and DEG promoters for specialist foragers vs. layers. **(A)** Motifs enriched within DAPs show maximum binding probabilities near peak summits. **(B)** Motifs enriched in promoter regions of forager>layer DEGs show elevated binding probabilities ~3kb upstream of and overlapping TSSs. Motif names and sequences are from FlyFactor (Zhu et al. 2011) for *Drosophila melanogaster*.

The relationship between TF activity and behavior was so strong that it was possible to predict individual behavior based solely upon the expression of TFs in the brain using a machine-learning algorithm and leave-one-out cross validation (Fig. 5A). TF expression correctly predicted 100% of foragers and 94% of layers. By contrast, it was not possible to predict generalists based on brain TF expression (only 1 of 8 correctly classified).

Brain GRN reconstruction (Chandrasekaran et al., 2011), performed on an individualized basis, further highlights the strong influence of gene regulatory plasticity on behavior. GRN activity was largely consistent between individuals within each behavioral group (Fig. 5B). Further, at the individual level, the activity of many TF modules (TFs and their predicted targets)

showed significant correlations with individual variation in several behavioral metrics, including numbers of eggs laid (50 TF modules), specialist behavioral score (77 TF modules), and number of foraging trips (74 TF modules) (File S8). At the individual level, 23 TF modules were correlated with all 9 behavioral and physiological metrics (Fig. S3, File S8). These behaviorally correlated TF modules include TFs involved in JH signaling (usp, Kr-h1, and Blimp-1), histone acetylation (trx), neuronal remodeling (Kr-h1, Hr51, trx), and circadian rhythms (opa and Hr51).

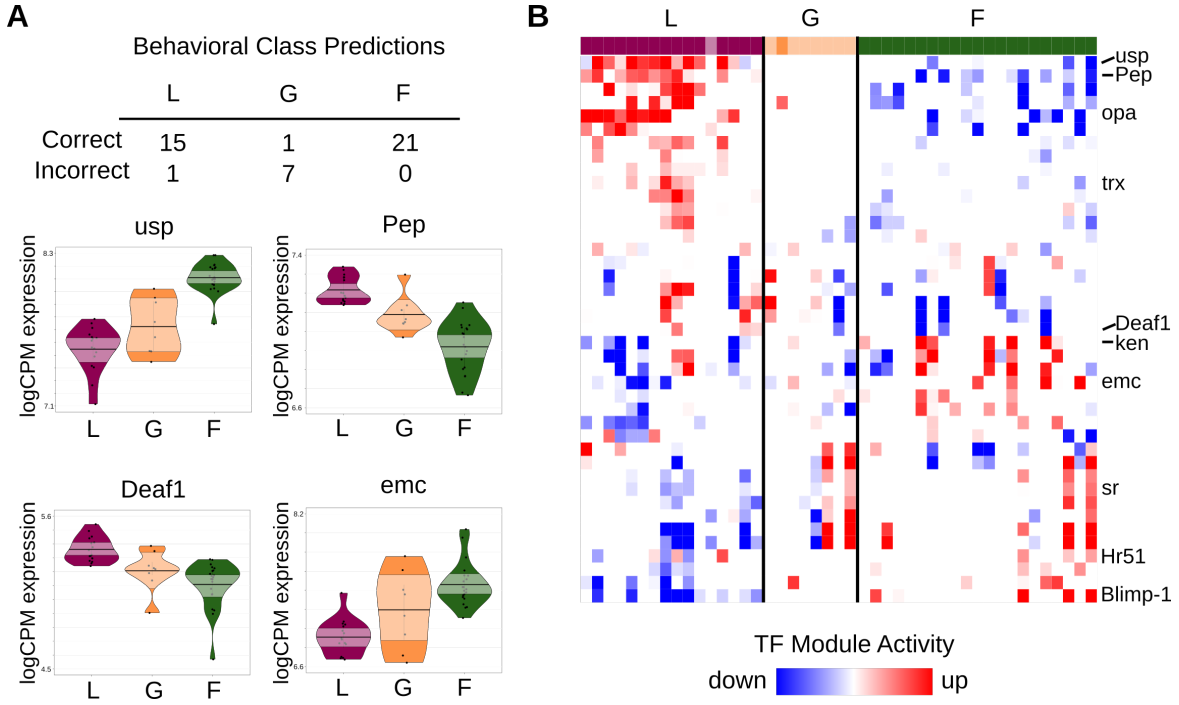

Figure 5. (A) Class prediction analysis based on brain TF expression correctly classified all but one specialist (L: layer, F: forager) but only one generalist (G). Normalized expression (logCPM) of 4 of the top 20 informative TFs for class prediction analysis are shown (others in Fig. S2). Median of points is represented by bold horizontal line within shaded 95% confidence interval, with length of shape and smoothed curve showing range and density of data, respectively. **(B)** TF modules (rows) with significant up/downregulation in at least 10 individuals, sorted by hierarchical clustering. Individuals (columns) are ordered by specialist score, with darkly colored blocks indicating correctly classified individuals based on TF expression prediction analysis and lightly colored blocks indicating incorrect classification. TF modules showed patterns of differentiation between L and F, while G were more variable in module activity. Labeled modules are those with TFs shown in panel (A) or discussed in text.

Comparative analyses of LW colony behavioral phenotypes and other social insect phenotypes

The performance of both egg laying and foraging by individuals in LW colonies, previously reported in Naeger et al. (2013), is unusual for honey bees; these behaviors are otherwise confined to separate castes (queens and workers). This raises the question of whether

283 the mechanisms underlying LW behavior reflect caste-related molecular differences. We
284 compared our gene expression results to previous studies of queens, workers, and worker
285 subcastes in various species of social insects to ask whether the molecular architecture of LW
286 phenotypes may be useful in the context of understanding additional social phenotypes.

287 In comparison with honey bee subcastes, forager-biased genes in LW colonies showed
288 significant overlap with forager-biased genes in two studies of queenright colonies (when
289 compared with nurses) (RF=1.7 p=1.707e-09; Alaux et al., 2009; RF=1.9 p=1.740e-07; Whitfield
290 et al., 2003; File S9). Layer-biased genes in this study overlapped with genes upregulated in
291 nurses relative to foragers in these queenright colonies (RF=1.7, p=3.656e-10; Alaux et al., 2009;
292 RF=2.0, p=1.116e-13; Whitfield et al., 2003; File S9).

293 In addition, differences in brain gene expression between egg-layers and foragers
294 mirrored caste-related differences across species. Genes differentially expressed between
295 foragers and egg-layers in this study were enriched for previously identified queen vs. worker
296 brain DEGs in *Megalopta genalis* bees, which facultatively engage in both reproductive and non-
297 reproductive behaviors (RF:1.3, p=0.009; Jones et al., 2017; File S9). Overlap was in the
298 expected direction, with queen-biased genes in *M. genalis* overlapping layer-biased genes
299 (RF:2.5, p=0.003) and worker-biased genes overlapping forager-biased genes (RF:1.6, p=0.01).
300 Further, worker-upregulated DEGs in the primitively eusocial wasp, *Polistes metricus*
301 overlapped significantly with forager-upregulated genes in this study (RF:2.6, p<0.0001; Toth et
302 al., 2010). In comparison with honey bee unmated queens and workers, overlap was significant
303 but in an unexpected direction: queen- and worker-biased genes overlapped with forager- and
304 layer- upregulated genes, respectively (RF:1.4, p=5.495e-08 and RF:1.2, p=0.008; Grozinger et
305 al., 2007; File S9).

306 Additionally, forager vs. layer DEGs in this study were enriched for genes identified as
307 under selection in two studies of social evolution. Forager vs. layer DEGs overlapped
308 significantly with genes undergoing positive selection in honey bees (RF=1.1, p=0.015; Harpur
309 et al., 2014; File S9) and across highly eusocial species relative to solitary or primitively eusocial
310 species (Woodard et al., 2011; File S9). Genes under selection in highly eusocial lineages were
311 enriched specifically for genes identified here as upregulated in foragers relative to layers
312 (RF=1.4, p=0.009), but not for layer-biased DEGs (p=0.106) (File S9). Forager vs. layer DEGs
313 were not significantly enriched for genes that were identified in a third study as under selection

314 in social lineages of bees (p=0.262; Kapheim et al., 2015; File S9). Many of the forager vs. layer
315 DEGs also found to be undergoing positive selection were related to metabolism (Fig. S4).
316
317 *TFs involved in LW plasticity previously implicated in social evolution*
318 Given that differences in brain gene expression between egg-layers and foragers reflect
319 caste-related differences, we also tested whether there is overlap between TFs involved in LW
320 plasticity and those previously implicated in social evolution. Indeed, many of the TFs we
321 identified above as related to behavioral plasticity based on motif enrichment, group predictive
322 analysis, or brain GRN activity were previously known to be associated with social behavior on
323 an evolutionary timescale. A comparative analysis of the genomes of ten bee species (Kapheim
324 et al., 2015) identified 13 TF motifs with associations between binding strength and social
325 complexity. Nine of those 13 motifs were also detected above as enriched within specialist DAPs
326 or DEG regulatory regions (p=0.015, hypergeometric test of overlap), and 6 of those 9 are
327 binding sites for TFs included in the above individualized GRNs. Along with TF module
328 correlation and behaviorally-predictive TF expression, these results highlight a set of 15 TFs as
329 compelling candidates in social plasticity and evolution, with significant associations in at least 3
330 of the 5 analyses (Fig. 6). The 15 TFs have functions related to known mechanisms associated
331 with social behavior, including brain development (Hamilton et al., 2016), JH signaling
332 (Woodard et al., 2011), and chromatin changes via histone acetylation (Simola et al., 2015).

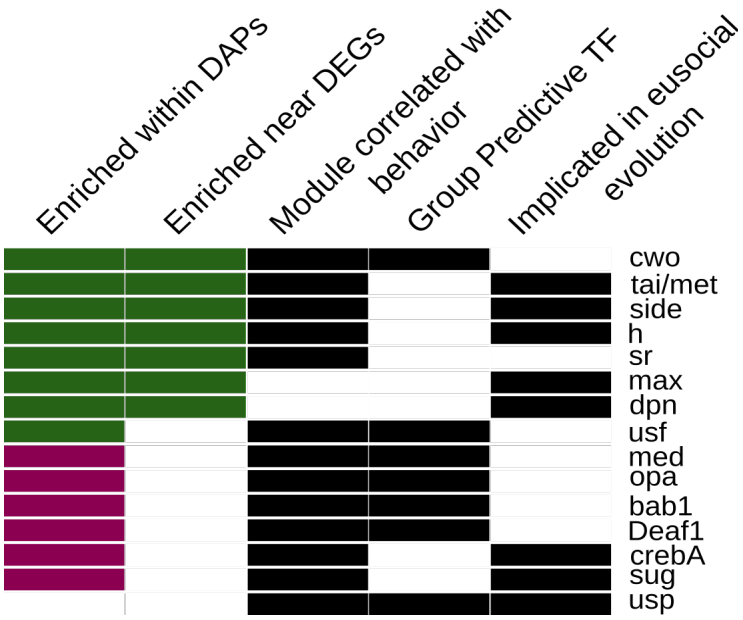

Figure 6. Candidate TFs regulating specialist behavioral phenotypes based on evidence across all analyses (descriptions of categories in Methods). Names given are for *Drosophila melanogaster* motifs (Zhu et al. 2011), with homology to honey bee genes as in Kapheim et al. (2015). Color of bar in first two columns indicates whether there was stronger enrichment among forager-biased (green) or layer-biased (purple) peaks or genes.

Discussion

Uncovering the regulatory mechanisms involved in behavioral plasticity is important to fully understand how behavioral phenotypes develop and evolve. We used automatic behavioral tracking and genomics to uncover the role of brain GRN activity in the extensive behavioral variation observed in colonies of laying worker honey bees. We discovered that continuous phenotypic variation is associated with continuous variation in both brain gene expression and brain chromatin accessibility, and that TF activity is predictive of behavioral phenotype at the individual level. These results provide new mechanistic insights into the important role played by brain GRNs in the regulation of behavioral plasticity, with implications for understanding the mechanisms and evolution of complex traits.

Our high-dimensional behavioral data revealed a near continuous distribution of phenotypes along an axis of egg-laying and foraging, two behaviors that are typically expressed separately in the queen and worker castes of honey bee colonies. Consistent with previous reports of ovary activation in queenless colonies (Page Jr and Erickson Jr, 1988; Sakagami, 1954), over half of workers tracked laid eggs. Some of these workers also engaged in foraging, consistent with the observations of Naeger et al. (2013), which supports the suggestion that some laying workers are not “selfish” reproducers but engage in activities that may benefit the colony

352 as a whole. We also showed a striking decoupling between ovary status and behavior, unlike in
353 many other social insect species (Barth et al., 1975; Michener, 1974; Wilson, 1971). Two-thirds
354 (14/21) of the foragers had activated ovaries, but most were infrequently predicted to lay eggs,
355 demonstrating that ovary activation alone is not a strong predictor of exactly which individuals
356 will lay eggs. This decoupling of reproductive physiology from reproductive behavior is
357 consistent with the evolutionary co-option of reproductive signaling pathways for non-
358 reproductive behaviors, a phenomenon well documented in honey bees (Amdam et al., 2008;
359 Graham et al., 2011; Page et al., 2012).

360 Like the task specialization observed in typical, queenright colonies of honey bees and
361 many other social insects (Oster and Wilson, 1979), the majority of individuals in LW colonies
362 showed consistency in performance of either egg-laying or foraging, but not both. Task
363 specialization can contribute to increased efficiency in social insects, either through learning or
364 reduction of task switching costs (Holldobler and Wilson, 1990; Jeanson et al., 2008; Trumbo
365 and Robinson, 1997; c.f. Dornhaus, 2008). In queenless colonies of honey bees, specialization
366 along a reproductive/non-reproductive axis may lead to increased production of haploid males
367 prior to the death of workers, with specialized foragers collecting food for these developing
368 drones while specialized egg-layers work to produce thousands of drones synchronously in these
369 terminal colonies (Page Jr and Erickson Jr, 1988). These findings suggest that LW honey bees
370 may display a form of colony organization that is adaptive, as opposed to one of chaos and
371 competition, which has long been thought to characterize LW colonies (Morse, 1990; Ratnieks et
372 al., 2006; Ratnieks and Wenseleers, 2008; Dadant & Sons, 1975; Wenseleers and Ratnieks,
373 2006). Worker derived drones have viable sperm (Gençer and Kahya, 2011) and therefore may
374 provide a permanently queenless honey bee colony with a final fitness opportunity if the males
375 can successfully mate with queens. It is difficult to evaluate this hypothesis because the
376 incidence of permanently queenless colonies is not known in natural populations of honey bees.
377 However, production of drones by workers in LW colonies is similar to that observed in bumble
378 bees, where worker competition over male production is a normal part of the colony cycle after
379 queen death (Cnaani et al., 2002; Free, 1955), or even prior to queen death in some species
380 (Velthuis and Duchateau, 2011).

381 Consistent with many other studies of behavior and brain gene expression across animal
382 species (e.g., Bukhari et al., 2019; Mello et al., 1992; Whitfield et al., 2003), we identified robust

383 brain transcriptional signatures associated with specific behavioral states. Beyond these group
384 level differences, we also discovered that large components of this molecular variation were
385 correlated with behavior at the individual level, and both behavior and brain gene regulatory
386 activity were continuous across bees. Our finding that both brain gene expression and chromatin
387 accessibility vary continuously with behavioral phenotype suggests that behavioral plasticity is
388 subserved by continuously varying molecular programs, rather than threshold-based or quantized
389 changes.

390 At the individual bee level, changes in the expression of TFs, accessibility of TF motifs
391 in enhancers and promoters, and activity of TF module target genes were all strongly associated
392 with behavioral state. This is highlighted by the results of our predictive analysis, where 97% of
393 specialists were accurately predicted to phenotype based on TF expression alone, despite the
394 small number of TFs relative to all differentially expressed genes. Spatial and temporal
395 integration of discrete events such as TF binding, aggregated at the whole brain level and across
396 TFs and genes, may lead to the continuous variation we observed in gene expression and
397 chromatin accessibility (e.g., Araya et al., 2014).

398 In addition to predicting the collective behavioral phenotypes of individual bees, our
399 analysis of GRNs allowed us to probe the influence of TF module activity on single behaviors.
400 We identified a set of 23 TF modules that were associated with all aspects of behavior and
401 physiology we measured. These TFs appear to coordinate sets of behaviors that are not overtly
402 linked (e.g., proportion of nectar foraging trips and number of eggs laid) but may be influenced
403 by the same regulatory machinery. Three of these modules are activated by TFs downstream of
404 JH, a hormone with numerous well-studied roles in social insect behavior, including the
405 regulation of oogenesis in queens and age-related division of labor in workers (Amdam et al.,
406 2008; Hamilton et al., 2017; Page et al., 2012). Our results are consistent with a role of JH
407 signaling in queenless colonies of worker honey bees, regulating a behavioral division of labor
408 between specialized egg-layers and foragers while also likely influencing ovary development and
409 oogenesis in the subset of individuals that lay eggs. These findings match previous work
410 describing differences in JH titers between egg-laying workers and foragers in queenless
411 colonies (Robinson et al., 1992), and suggest that mechanisms underlying variation in egg-laying
412 behavior may be similar to nurse/forager differences in queenright colonies. Overlap in brain
413 gene expression profiles between nurses and egg-layers further supports this conclusion.

While behavioral specialization appears to be common among members of queenless honey bee colonies, the finding of even a small number of generalist bees who perform both egg-laying and foraging has intriguing implications. The presence of these generalists suggests that despite the long divergence from a solitary ancestor (~85 my, Branstetter et al., 2017), honey bees retain great flexibility for performance of multiple behaviors that are typically confined to either the queen or worker caste. Latent plasticity in social insects that is inducible under extreme conditions is also seen in morphologically and temporally defined worker subcastes (Robinson, 1992; Simola et al., 2015; Wilson, 1980). Generalists showed high variation in behavior, and similarly were difficult to predict phenotypically based on TF activity, unlike specialists. Further, brain GRN activity in these individuals was less defined, with fewer TF modules showing significant up- or down-regulation in generalist individuals compared with specialists. Combined with PCA on brain gene expression and chromatin accessibility, these findings suggest that generalists are molecularly intermediate between specialized groups.

Our discovery of intermediate generalist phenotypes in laying worker colonies provides molecular support for one of the leading theories of eusocial evolution, the Ovarian Ground Plan Hypothesis (OGPH). The OGPH posits that the emergence of queen and worker castes from solitary ancestors involved the genetic decoupling of reproductive and non-reproductive behavioral programs through changes in gene regulation acting on ancestral plasticity (Gadagkar, 1997; Turillazzi and West-Eberhard, 1996; West-Eberhard, 1987). The phenotypic continuum we observed in laying worker colonies, with both reproductive and non-reproductive specialists as well as generalists, suggests that this decoupling process is at least partially reversible and/or incomplete in honey bees, unlike in eusocial species where workers lack reproductive anatomy and corresponding behaviors entirely (e.g., ants and higher termites). Additionally, molecular characterization of this behavioral variation, especially our TF analyses, supports the hypothesis that incremental changes in gene regulatory network activity led to the decoupling of solitary behavioral programs into distinct queen and worker castes. This hypothesis is consistent with previous research linking changes in TF activity with social evolution (Kapheim et al., 2020, 2015). If correct, this hypothesis provides a framework for understanding the evolution of eusociality at the molecular level.

Methods

Bees and colony setup

Source colonies

Honey bee colonies were maintained according to standard beekeeping practices at the University of Illinois Bee Research Facility in Urbana, Illinois. One-day-old adult worker bees were obtained by removing sealed honeycomb frames of late-stage pupae from source colonies in the field and housing them in an incubator inside emergence cages at 34 °C and 50% relative humidity. Bees were removed from frames daily to collect adults less than 24 hours old.

Prior to establishing the colonies of barcoded bees, 16 source colonies were screened for worker egg-laying ("laying worker", LW) potential by stocking Plexiglas cages with 50-100 one-day-old workers and holding them in queenless, broodless conditions. Cages contained small pieces of 3D-printed honeycomb (similar to Fine et al., 2018) to provide a standardized location for workers to lay eggs, as well as 50% sucrose solution and pollen paste (45:45:10 ratio by weight of pollen, honey, and water) provided ad libitum and refreshed daily. Cages were monitored daily to count eggs. We found, as in other studies, variation in the timing and extent of LW development among different source colonies (Fig. S5), reflecting the effect of genotypic and/or environmental differences on laying worker potential (Miller III and Ratnieks, 2001; Page and Robinson, 1994; Robinson et al., 1990; Velthuis, 1970). When possible, source colonies were chosen from among those screened that displayed high levels of worker egg-laying in cages within 14 days.

To reduce genetic variation among bees used for sequencing, experimental colonies D-F were established from a mix of two source colonies each headed by a queen of either *Apis mellifera ligustica* or *Apis mellifera carnica* origin who had been artificially inseminated with semen from a single drone (SDI) (queen rearing and inseminations performed by Sue Cobey, Honey Bee Insemination Service; Washington State University; US stocks of bees are primarily, but not completely *ligustica* or *carnica*). Experimental colonies A-C were established from naturally mated, *Apis mellifera ligustica* source colonies. Honeycomb frames of late-stage pupae were removed from source colonies and maintained in an indoor incubator. Worker bees were collected from these frames each day to obtain 0-24 hr old individuals for barcoding. A total of 800 bees were used for each experimental colony, collected and barcoded over 1-2 days upon eclosion (File S10).

475 Barcoding bees

476 Bees were tagged with "bCode" barcodes as in Gernat et al. (2018). Unique sets of
477 bCodes were used to differentiate bees barcoded on different days, as well as to differentiate bees
478 from different source colonies in colonies D-F. To attach bCodes to bees, workers were
479 anesthetized on ice and then positioned using soft forceps (BioQuip, Compton, CA). A small
480 drop of Loctite Super Glue Gel Control (Henkel, Düsseldorf, Germany) was applied to the center
481 of the thorax of each bee, followed by a bCode positioned with its left and right edge parallel to
482 the anteroposterior axis of the bee. Bees were carefully placed in plastic dishes until they
483 recovered from cold anesthetization, at which point the glue was dry. After waking, all bees were
484 placed in a large container with Fluon®-coated walls (Insect-a-Slip, BioQuip) where honey was
485 provided *ad libitum* until placement into a custom observation hive, described below. At the end
486 of each barcoding day, bees were carefully transferred into the observation hive.
487
488 *Behavioral tracking*

489 Hive monitoring

490 Barcoded bees were housed in a glass-walled observation hive with a one-sided plastic
491 honeycomb frame, as in Gernat et al. (2018). Bees were unable to access the back side of the
492 honeycomb, and could exit the hive through a plastic tube to the outside. Colonies were
493 maintained in a dark room with a heater and humidifier that kept the room at approximately 32°C
494 and 50% relative humidity.

495 Infrared light (not visible to bees) was used to illuminate the hive from both the front and
496 back while capturing hive images. Images were acquired at one-second resolution with a
497 monochrome Prosilica GX6600 machine vision camera (Allied Vision, Stadtroda, Germany) fitted
498 with a Nikkor AF 135 mm f/2 D DC prime lens (Nikon, Minato City, Japan). Additional details
499 about image acquisition can be found in Gernat et al. (2018). Images were saved to a redundant
500 array of independent disks, then copied onto a computing cluster (Biocluster, UIUC) for analysis
501 after the end of each experimental recording period.

502 Entrance monitoring

503 Colonies of barcoded bees were given access to the outside via a tube connected through
504 an exterior wall of the Bee Research Facility to an entrance equipped with an automated flight
505 activity monitor as in Geffre et al. (2020). This monitor included a maze to slow down incoming

506 and outgoing bees, and a Raspberry Pi camera (5 megapixel v1.3, Adafruit, New York, NY) that
507 imaged the maze twice per second from 07:00 until 19:00 daily. The camera was controlled by a
508 Raspberry Pi 2B computer running the Raspian 8 operating system, using a custom shell script and
509 the raspistill program to record images.

510 *Barcode detection*

511 Barcodes were detected in hive images as in Gernat et al. (2018) and filtered to facilitate
512 subsequent behavioral analyses. Filtering involved removal of potential tracking errors, including
513 removal of barcodes that did not pass read error correction. In addition, records for barcodes that
514 were read twice in the same image were removed, as were hive image records of the same barcode
515 identified more than 5 cm/second between successive detections, which are likely to be
516 misidentifications. An average of 94.51% of detections remained after these filtering steps (range
517 across colonies: 91.94-97.11%). Finally, the time of death of each bee was estimated using the last
518 time she was observed for at least 4 minutes during a 5-minute window above the third row of
519 honeycomb cells from the bottom of the hive; dead bees tend to accumulate below this level prior
520 to being removed by other bees (Gernat et al., 2018). Records for bees following their time of
521 death were filtered out so behavioral scores (below) were calculated only over times in which bees
522 were alive.

523 In entrance monitor images, barcodes were similarly detected as in hive images, but with
524 parameters adjusted for images produced by the Raspberry Pi camera. Fast-moving bees were not
525 filtered out in entrance images, because bees do move quickly through the entrance monitor and
526 due to the relatively small number of bees that fit into the maze, spurious fast movement due to
527 bCode decoding errors is unlikely.

528 *Egg-laying detector*

529 <u>Annotated image library</u>

530 Hive images from three experimental colonies and across 12 different days were used for
531 manual annotation of egg-laying events. The software Fiji (Schindelin et al., 2012) was used to
532 mark the bCode positions of all workers laying eggs in an initial set of 1500 hive images, followed
533 by an additional set of 782 images, each annotated by three independent observers. After the initial
534 identification of egg-laying bees in these images, the two seconds before and after each egg-laying

event were also annotated for those bees. Bees not marked as laying eggs with visible bCodes were considered non-egg-laying for training of the CNN, below.

CNN training and performance estimation

Two convolutional neural networks (CNNs) were trained on the annotated egg-laying images, using TensorFlow™ (Abadi et al., 2016). The first CNN used images cropped to include just a small rectangular region behind the barcode of each bee. For egg-laying bees, these images show the honeycomb, because their abdomen is backed into the comb and thus not visible. For non-layers, these images show the abdomen. The CNN was trained to differentiate between these two cases. The second CNN was applied to images of bees that were identified as potential egg-layers by the first CNN. It used slightly larger images that showed the entire bee and was trained to use information about the bee's posture and her immediate surroundings to identify false positives, which were subsequently filtered out.

Application of a CNN to an image results in a score between 0 and 1 that reflects the likelihood of that image showing the event of interest. Deciding whether a score is sufficiently high for assuming that the event took place involves thresholding that score. To choose thresholds for each CNN score and a minimum egg-laying duration, a calibration set of images, which were not used for training the CNNs, was used to estimate the performance of the egg-laying detector for different threshold combinations. Thresholds were chosen from this calibration set to maximize the detector's positive predictive value, then were applied to an independent test set of images that had also never been seen by the detector to obtain unbiased performance values. Based on the performance estimation on the test set of images, the egg-laying detector had the following performance: 99.71% accuracy, 35.39% sensitivity, 100% specificity, 100% positive predictive value, and 99.71% negative predictive value. Minimizing false positives came at a cost to sensitivity, but bees who lay eggs will likely do so more than once over the course of the experiment and can thus still be identified as egg-layers (honey bees possess multiple ovarioles, each of which can develop eggs simultaneously (Hess, 1942)). Egg-laying detections were further aggregated into events: subsequent detections that occurred within 10 seconds and 11.2 mm (the width of two honeycomb cells) of one another were assumed to belong to the same egg-laying event and were merged.

Filtering and annotation of entrance data

Raw detections of bees in the entrance were filtered as in Geffre et al. (2020). Briefly, a bee must traverse at least one-third the distance of the entrance monitor to be counted, and traversals that occurred within 10 seconds of each other were merged into a single event. These traversal events were then determined to be incoming or outgoing based on the positional coordinates of the bee at the start and end times of each event. Numbers of foraging trips (File S1) was inferred from series of outgoing and incoming events.

Incoming foraging trips were additionally annotated with trophallaxis data to determine whether a forager likely returned with nectar. CNNs trained to identify pairs of bees engaged in trophallaxis as well as the direction of trophallaxis (i.e., which bee was donor and which was recipient; Gernat et al., unpublished) were used to annotate incoming trips for all bees. Parameters used for the detector resulted in the following performance metrics based on test images: 88.7% sensitivity, 99.6% specificity, 90.4% positive predictive value, 99.6% negative predictive value, and 88.9% accuracy in determining trophallactic role (donor or receiver) of each bee. If a bee was a trophallaxis donor within 5 minutes after returning from a trip (Seeley, 2009), with no trophallaxis reception prior to the donation, that foraging trip was annotated as a nectar trip. Additionally, incoming trips were manually annotated for pollen on the hindlegs of returning bees for colonies D-F. Combining these nectar and pollen data for each trip, the proportion of foraging trips with nectar ("p.nectar"), pollen ("p.pollen") or both ("p.both") were calculated per bee in these colonies.

Specialist and generalist scores

In order to characterize the activity of egg-laying and foraging for each bee, two behavioral scores were created. The "specialist" score describes how specialized an individual was on either egg-laying (scores near -1) or foraging (scores near +1) relative to other bees in the colony; bees that consistently performed both egg-laying and foraging, or that performed neither behavior, have specialist scores near 0. The generalist score ranges from 0 to 1 and describes the degree to which an individual performed both egg-laying and foraging behaviors, differentiating bees with specialist scores near 0 based on the performance (or not) of egg-laying and foraging. Scores were created by first counting the number of egg-laying and foraging events per day. Bees were then ranked for each behavior relative to other bees in the colony on the same day, with tying ranks being assigned the minimal rank (e.g., if three bees were tied between the 4th and 8th ranked bees,

they all received a rank of 5). Ranks were then normalized by dividing by the maximum rank, so that all ranks were in the range [0,1]. The normalized rank space for each bee (i.e., normalized egg-laying rank and normalized foraging rank) was then mapped to behavioral scores (and corresponding color space) using the following formulae in polar coordinates (ρ,Θ) on the two-dimensional rank space: generalist score = $(1/2)\rho^2\sin^4 2\Theta$, specialist score= $\sin(\Theta-\pi/4)\rho^4\cos^4 2\Theta$. Note that the numerical value of the scores has no biological meaning, but is simply a mapping from rank space to the space of colors as shown in Fig. S6.

Selection of bees for sequencing

The median of specialist and generalist scores was weighted to emphasize the latter part of the experiment; days 15-21 received a weight of 1-7, respectively, and each day's score was multiplied by this weight. These scores were used to characterize the overall behavior of each bee in the colony. The rank approach allowed for normalization across days with different overall levels of activity in the colony, and the median score across days provides an overall assessment of the lifetime behavior of each bee. These weighted median scores were used to rank all bees, and the top ranking specialists and generalists from two colonies were selected for brain RNA sequencing (RNAseq) and Assay for Transposase-Accessible Chromatin using sequencing (ATACseq). Scores for each sequenced bee (n=45, 25 from colony E, 20 from colony F), as well as total numbers of detected egg-laying and foraging events per bee, are provided in File S2.

To examine variation in behavior within and among groups, principal component analysis (PCA) was performed on the following set of behavioral traits (see also File S2): number of eggs laid, number of foraging events, proportion of trips with evidence of nectar collection, proportion of trips with evidence of pollen collection, and proportion of trips with evidence of both nectar and pollen. PCA was performed in R using the prcomp function and plotted using the ggplot2 package.

Tissue dissection and homogenization

At the end of behavioral tracking, bees were collected from each colony and stored at -80°C. For bees selected for sequencing, abdomens of each bee were carefully removed on dry ice and incubated for 16 hours at -20°C in RNA-later ICE (Life Technologies, Carlsbad, CA). Ovaries were imaged and assessed for ovary development using a 1-5 scale adapted from (Hess, 1942) to assign an ovary score; a score of 3-5 indicates ovary activation. These dissections confirmed that

624 egg-layers and generalists had activated ovaries, while many foragers did not. Ovary scores, as
625 well as number of ovarioles as determined from dissections, are given in File S2.
626 The head of each bee was freeze-dried at 300 milliTorr for 55 minutes, and whole brains
627 were removed from the head capsule in a dry ice ethanol bath (Schulz and Robinson, 1999).
628 Dissected brains were stored individually in 1.5 mL microcentrifuge tubes at -80°C until
629 extractions.
630 Brains were individually homogenized in 150 µL phosphate buffered saline (1X PBS,
631 Corning, Corning, NY, cat. #21-040-CV) with protein inhibitor complex (PIC, Complete Tablets,
632 EDTA-free Protease Inhibitor Cocktail from Roche, Basel, Switzerland, cat. #04693132001) using
633 a motorized pestle for 20 seconds. 50 µL of this homogenate was then pipetted into 450 µL cold
634 PBS+PIC and placed on ice for ATAC-seq library preparation (see below). The remaining 100 µL
635 homogenate was mixed with 500 µL RLT buffer (Qiagen, Hilden, Germany) with 1% β-
636 mercaptoethanol for use in the Qiagen RNeasy Mini Kit RNA extraction protocol (see below).

637 *RNAseq library preparation and sequencing*

638 Whole brain RNA was extracted from the 600 µL homogenate in RLT buffer after an
639 additional 30 second homogenization following the Qiagen RNeasy Mini Kit protocol, including
640 a DNase (Qiagen) treatment to remove genomic DNA. RNA quantities were determined for each
641 sample using a Qubit RNA HS Assay Kit (Invitrogen, Carlsbad, CA). High RNA integrity for all
642 samples was confirmed with Bioanalyzer 2100 RNA Pico chips (Agilent, Santa Clara, CA) prior
643 to library preparation.
644 RNAseq libraries were constructed and sequenced by the W.M. Keck Center for
645 Comparative and Functional Genomics at the Roy J. Carver Biotechnology Center (University of
646 Illinois at Urbana-Champaign). Libraries were constructed from 500 ng RNA per sample using the
647 TruSeq Stranded mRNA HT kit (Illumina, San Diego, CA) on an ePMotion 5075 robot
648 (Eppendorf, Hamburg, Germany). Libraries were uniquely barcoded, quantified, and pooled for
649 sequencing across 6 lanes with 100 nt single-end sequencing on the Illumina HiSeq 4000.

650 *ATACseq library preparation and sequencing*

651 The 500 µL tissue homogenate was additionally homogenized by aspirating through a 20
652 gauge needle followed by a 23 gauge needle 5 times each. Samples were centrifuged at 500g for
653 5 minutes at 4°C. Supernatant was removed, and cells were resuspended in 50 µL cold PBS+PIC.

654 15 µL of this cell suspension (approximately 1/10th of the total brain, ~100k cells) was placed into
655 a new microcentrifuge tube, and this was centrifuged at 500g for 5 minutes at 4°C as an additional
656 cell washing step. Supernatant was removed, and cells were gently resuspended in 50 µL cold lysis
657 buffer prepared as in Buenrostro et al. (2015). The remainder of the ATACseq library protocol
658 followed Buenrostro et al. (2015), with the exception of the final purification step, where a 0.8:1
659 ratio of Ampure XP beads (Beckman Coulter, Brea, CA) to sample was used to purify each library.
660 In addition to sample libraries, input libraries were constructed from thoracic genomic DNA from
661 a random bee from each colony per sequencing batch using 50 ng of genomic DNA (extracted
662 using the Gentra Puregene Tissue Kit from Qiagen, cat. #158667, following manufacturer's
663 protocol for DNA purification from 25 mg tissue but with 6 µL proteinase K and 4 µL RNase A
664 at the appropriate steps). Genomic DNA was transposed with Nextera Tn5 Transposase (Nextera
665 Kit, Illumina) following the ATACseq protocol immediately following the cell lysis step
666 (Buenrostro et al., 2015), again using an 0.8:1 Ampure XP bead clean-up at the end of the protocol.
667 A Qubit dsDNA HS Assay Kit (Invitrogen) was used to quantify each library, and library size and
668 quality was assessed using a Bioanalyzer High-Sensitivity DNA Analysis kit (Agilent).
669 ATACseq libraries, including input libraries, were pooled at equal nM concentrations and
670 a bead clean-up (0.8:1 ratio of Ampure XP beads to sample) was performed on the pool prior to
671 submission for sequencing. QC on the final pool was performed using qPCR and an AATI
672 Fragment Analyzer by the Keck Center. Libraries were sequenced across three lanes with 100 nt
673 paired-end sequencing on the Illumina HiSeq 4000 by the Keck Center.

674 *Data processing and analysis*

675 <u>RNAseq</u>

676 Sequencing of RNAseq libraries (n=45, 25 from colony E, 20 from colony F) produced
677 1,487,641,973 reads which survived quality and adapter trimming using Trimmomatic (version
678 0.36, parameters used: ILLUMINACLIP: 2:35:30 LEADING:20 TRAILING:20 MINLEN:30).
679 Trimmed reads were aligned to the *Apis mellifera* HAv3.1 genome (NCBI accession
680 GCA_003254395.2) using STAR (version 2.5.3) and default parameters, resulting in an average
681 of 96.7% reads mapping uniquely. The program featureCounts from the Subread package (version
682 1.5.2) was used to assign mapped reads to gene features from the GFF file from NCBI associated
683 with the *A. mellifera* HAv3.1 genome. On average, 84.8% of uniquely mapped reads were assigned
684 to gene features using featureCounts.

685 Gene counts were imported into R for differential expression analysis using edgeR. Genes
686 with less than 1 CPM in at least 2 samples were removed, and remaining count values were
687 normalized using the TMM method. Gene-wise variances were calculated by estimating tagwise
688 dispersions in edgeR on filtered gene count matrices for each group separately and plotted using
689 ggplot2. Tagwise dispersion estimates were followed by quasi-likelihood F-tests for each pairwise
690 comparison of groups. Differentially expressed genes (DEGs) for each pairwise comparison are
691 given in File S3.

692 ATACseq

693 ATACseq libraries (n=48, 25 from colony E, 20 from colony F, 3 input libraries) produced
694 1,110,401,018 paired-end reads which survived quality and adapter trimming using Trimmomatic
695 (version 0.38, parameters used: ILLUMINACLIP: 2:15:10 HEADCROP:10 LEADING:20
696 TRAILING 20 SLIDINGWINDOW:4:15 MINLEN:30). An average of 98.1% of reads mapped to
697 the *Apis mellifera* HAv3.1 genome using bwa mem (version 0.7.17, default parameters).
698 Duplicates were marked and removed prior to further processing using picard (version 2.10.1,
699 average duplication level 30.2%).

700 Peaks were called from deduplicated BAM files using MACS2 (version 2.1.1, command:
701 callpeak, with parameters: --nomodel -g 2.5e8 --nolambda --keep-dup all --slocal 10000) using the
702 appropriate colony and sequencing batch input as control. Peaks were called on each colony and
703 behavioral group separately, then merged and sorted using BEDTools (version 2.26.0, sort and
704 merge commands). This resulted in a total of 11,614 merged peaks with an average width of 721
705 bp. Mapped reads were counted to each peak per individual using featureCounts from the Subread
706 package (version 1.5.2). An average of 51.0% of reads were mapped to called peaks.

707 Peak counts were imported into R for differential accessibility analysis using edgeR. Peaks
708 with less than 1 CPM in at least 2 samples were removed, and remaining count values were
709 normalized using the TMM method. Gene-wise variances were calculated by estimating tagwise
710 dispersions in edgeR on filtered gene count matrices for each group separately and plotted using
711 ggplot2. Tagwise dispersion estimates were followed by quasi-likelihood F-tests for each pairwise
712 comparison of groups. Differentially accessible peak (DAP) results for each pairwise comparison
713 are given in File S4.

714 *Functional annotation of differential expression and chromatin accessibility*

715 Differential expression

716 Differentially expressed gene (DEG) lists were functionally annotated using Gene
717 Ontology (GO) by first mapping putative orthologs between *Apis mellifera* and *Drosophila*
718 *melanogaster* using reciprocal best BLASTP hits (e-value cutoff = 1e-5). Only DEGs with putative
719 *D. melanogaster* orthologs were included for GO enrichment, and the background list used was all
720 tested genes (those which passed the minimum expression threshold) with putative *D.*
721 *melanogaster* orthologs. Enrichment tests for biological processes were conducted using GOrilla
722 (Eden et al., 2009) with all significant DEGs (FDR-corrected p-value<0.05) against the
723 background list. GO enrichment results for all DEG lists are given in File S3.

724 Differential accessibility

725 To functionally annotate DAPs, the midpoint coordinate of the 11,614 peaks identified with
726 MACS2 were assigned to genes based on proximity to honey bee gene features (*Apis mellifera*
727 HAv3.1 genome). The following features were considered per gene: promoters (1 kb upstream),
728 introns, exons, 5' UTR, 3' UTR, upstream (10 kb upstream), and downstream (10 kb). Peaks not
729 associated with any gene feature were classified as intergenic. When peaks were associated with
730 multiple genes (e.g., the intron of one gene and the promoter of another), they were assigned to
731 individual genes based on the following priority: promoter (highest priority), exon, 5' UTR, 3'
732 UTR, intron, upstream, downstream (lowest priority). If a peak was present in the same highest
733 priority class for multiple genes, it was randomly assigned to one gene. In this way, each peak was
734 assigned to either a single gene or considered intergenic. Of the 11,614 peaks, 1822 were assigned
735 to the promoter region of a gene, 776 to exons, 1326 to 5' UTRs, 273 to 3' UTRs, 4666 to introns,
736 1155 to upstream regions, 773 to downstream regions, and 823 peaks were located in intergenic
737 regions.

738 As before with GO enrichment for DEGs, Differentially accessible peaks (DAPs) were
739 functionally annotated by mapping peak-associated genes to putative orthologs in *D. melanogaster*
740 using BLASTP. The background list for enrichment analyses was the list of peaks which met the
741 minimum accessibility count threshold for analysis and which had putative orthologs in *D.*
742 *melanogaster.* GOrilla (Eden et al., 2009) was used for enrichment tests. GO enrichment results
743 for all DAP lists are given in File S4.

744 *Motif enrichment of DAPs and DEG regulatory regions*

745 Transcription factor (TF) motif enrichment analysis in this study was performed similarly
746 to the methods described in Whitney et al. (2014). The overall approach is as follows, with details
747 below. For each TF motif, 1) genomic windows were scored for the presence of the motif, 2)
748 window scores were combined into scores for genomic segments of interest, representing either
749 gene regulatory regions or accessibility peaks, 3) a set of motif targets was created using a fixed
750 cutoff on the segment scores, and 4) a statistical test for enrichment was performed between
751 segments that were motif targets and those that were significant in differential analysis.

752 Motif scores for genomic windows

753 First, we divided the honey bee genome (version HAv3.1, NCBI accession
754 GCA_003254395.2) into 500 bp windows with 250 bp shifts. We gathered a collection of 223
755 representative TFs (Kapheim et al., 2015) and downloaded their DNA binding specificities
756 (motifs) characterized as position weight matrices (PWMs) from FlyFactorSurvey (Zhu et al.,
757 2011). Separately for each TF motif, we ran the Stubb algorithm (Sinha et al., 2003) on all genomic
758 windows to score them for the presence of that TF's binding sites. Tandem repeats in the windows
759 were masked using the Tandem Repeat Finder (Benson, 1999) before calculating the Stubb scores
760 to avoid scoring the repeats as weak binding sites. Since the honey bee genome has significant
761 local G/C heterogeneity (Sinha et al., 2006), we converted the raw Stubb scores for each window
762 into G/C content-normalized empirical p-values. This was done by determining the rank of each
763 window among all genomic windows of similar G/C content (when grouped into 20 G/C bins).

764 Scores for genomic segments

765 We defined two different collections of genomic segments (accessibility peaks and gene
766 regulatory regions) to analyze with motif enrichment in this study. Since the genomic segments
767 may overlap with a variable number of our genomic windows, we defined a length-adjusted motif
768 score for each segment. This score was calculated using the score of the best scoring window in
769 that segment for the given motif and the number of windows overlapping the segment, as follows:

770 $$sc_{seg} = 1 - (1 - pval_{best})^N$$

771 where,

772 sc_{seg} = *length-adjusted motif score for the segment*

773 *N = number of windows that overlap with the scoring window*

774 $pval_{best}$ *= best G/C normalized empirical p-value among the N overlapping windows.*

775 Statistical test for TF enrichment

776 TF enrichment was analyzed for two sets of regions: DAPs (Differentially Accessible
777 Peaks) and DEGs (Differentially Expressed Genes) (File S7).

778 For analysis of DAPs, the collection of genomic segments was defined as the combination
779 of all DAPs and randomly selected non-accessible parts of genome that had the same distribution
780 of lengths as those DAPs. The number of randomly selected genomic segments was set to 10 times
781 the number of DAP segments. For each motif, the top 200 scoring segments from the collection
782 were defined as the TF motif target set. Hypergeometric p-values were calculated for each motif-
783 DAP set pair (File S7) to quantify the significance of the overlap between the corresponding TF
784 motif target set and DAP set.

785 For DEGs, the collection of genomic segments was the regulatory regions of all genes in
786 the honey bee annotation (Amel_OGSv3.21). Each regulatory region was defined as 5kb upstream
787 to 2kb downstream of the transcriptional start site of its gene
788 (http://veda.cs.uiuc.edu/beeMotifScores/). The top 500 scoring segments from the gene universe
789 were selected as the TF motif target set for each motif. Finally, the significance of the overlap for
790 each motif-DEG set pair (File S7) was calculated with the Hypergeometric p-value.

791 All p-values were then converted to q-values using the "qvalue" function in the R software
792 package qvalue (Storey et al., 2019) to control the false discovery rate from multiple hypothesis
793 testing.

794 For motifs enriched both within DAPs and DEG upstream regions, CentriMo (Bailey and
795 Machanick, 2012) from MEME Suite was used to calculate and plot the probability of motif
796 binding across 2 kb windows centered on the peak summit for DAPs and 7 kb windows (5kb
797 upstream and 2kb downstream of the transcriptional start site (TSS)) for DEGs. These probabilities
798 are shown in Fig. 4.

799 *Individualized Gene Regulatory Network (GRN) analysis*

800 To understand how TFs orchestrate transcriptional changes in the brain, we reconstructed
801 a gene regulatory network (GRN) model using the ASTRIX approach (Chandrasekaran, 2014;

802 Chandrasekaran et al., 2011). ASTRIX uses gene expression data to identify interactions between
803 TFs and their target genes. The ASTRIX algorithm has been previously used to infer brain GRN
804 models for various organisms including the honey bee (Bukhari et al., 2017; Saul et al., 2017;
805 Shpigler et al., 2017). These models showed significantly high accuracy in predicting gene
806 expression changes in the brain and identified TFs that regulate social behaviors.

807 Here we applied ASTRIX using the gene expression data of the 45 individual bees along
808 with a list of honey bee TFs as input to identify regulatory interactions. We normalized the
809 transcriptomics data prior to GRN construction using the ComBat algorithm (Johnson et al., 2007)
810 to minimize batch and colony effects in the data. The effectiveness of the normalization was
811 checked using PCA. Any TF predicted to interact with a given target gene by ASTRIX had to pass
812 through two criteria: 1) share a significant degree of mutual information with the target gene (p-
813 value $< 10^{-6}$), and 2) explain at least 10% of the variance of the target gene, quantified by Least
814 angle regression algorithm. Similarly, each target gene included in the GRN must be predicted
815 with a correlation of at least 0.8 by the ASTRIX model using expression levels of TFs.

816 The GRN model built by ASTRIX predicted 2,190 genes with a Pearson's correlation of
817 0.8 or higher using expression levels of TFs. Overall, the GRN inferred by ASTRIX contains 4,500
818 interactions between 190 TFs and the 2,190 target genes. The full GRN is in File S8.

819 To determine TFs correlated with specific behaviors, we first identified genes that were
820 strongly correlated with specific behavior scores across all individuals (FDR p-value of correlation
821 < 0.001). TFs whose targets were over-represented among the behavior-correlated genes were then
822 determined. Significance of the overlap between the list of behavior-correlated genes with targets
823 of each TF ("TF module") was estimated using the hypergeometric test.

824 Finally, to identify TF modules associated with expression changes in each individual
825 ("Individualized TF modules"), genes that were upregulated or downregulated in each individual
826 were identified using z-transformation. Genes in each individual with z-scores above 2 (i.e., 2
827 standard deviations above mean) or below -2 were considered to be differentially expressed in an
828 individual. This list of genes was then overlapped with TF modules to identify modules
829 significantly associated with each individual using the hypergeometric test of overlap.

830 We used a Random Forests classification algorithm for predicting individual behavioral
831 group from TF expression levels. A leave-one-out cross validation analysis was performed wherein
832 the algorithm was trained using data from the remaining 44 individuals and then used to predict

833 the behavior of the 45th individual using its TF levels. The model achieved an accuracy of 82% in
834 predicting behavior. Performance of the model was evaluated by comparison with random
835 shuffling of the behavior labels. We made predictions 100 times with a different set of shuffled
836 labels and compared the accuracy of predictions (i.e., total individuals for which behavioral group
837 was correctly predicted) between the random model and the Random Forest algorithm using a t-
838 test ($p=1 \times 10^{-8}$). This suggests that TF expression levels can accurately forecast the behavior of
839 the individual, especially for specialists. The relative importance of each TF in predicting behavior
840 was determined using Out-of-bag predictor importance estimation, wherein each predictor's value
841 is permuted and the corresponding impact on model accuracy is determined (importance scores
842 given in File S8). The random forest classification algorithm was implemented in MATLAB with
843 default parameters for the number of predictors sampled (square root of the number of predictors,
844 in this case 258 TFs) and default values for the tree depth (n - 1, where n is the training data size).

845 *Selection of candidate TFs involved in specialized phenotypes*

846 Candidate TFs displayed in Fig. 6 were drawn from multiple analyses presented in this
847 paper and in Kapheim et al. (2015). "Enriched within DAPs" indicates enrichment of the TF motif
848 within forager vs. layer DAPs from the analysis of ATACseq data within this manuscript (see
849 *Motif enrichment of DAPs and DEG promoters* and File S7*)*. Similarly, "Enriched near DEGs"
850 indicates enrichment of the TF motif among putative regulatory regions of forager vs. layer DEGs
851 (see *Motif enrichment of DAPs and DEG promoters* and File S7*)*. "Module correlated with
852 behavior" indicates that TF module expression is significantly correlated with at least one
853 behavioral metric across individuals (see *Individualized Gene Regulatory Network (GRN) analysis*
854 and File S8). "Group Predictive TF" indicates the TF is among the 20 most informative for
855 predicting individual group membership based on TF expression (see *Individualized Gene*
856 *Regulatory Network (GRN) analysis* and File S8). "Implicated in eusocial evolution" indicates that
857 the TF motif was previously found to be associated with social evolution in Kapheim et al. (2015).
858

859 **Acknowledgements**

860 We thank A. Sankey, A. Ray, S. Bransley, J. Cullum, K. Wilk and J. Falk for assistance
861 in the field, A. Hernandez and the staff at the Carver Biotechnology Center for sequencing
862 services, administrators of Biocluster (UIUC) for computational support, and M.B. Sokolowski,
863 M. Hudson, A.M. Bell, members of the Robinson lab, and three anonymous reviewers for

comments that improved this manuscript. Funding: This research was supported by Grant R01GM117467 from the National Institute of General Medical Sciences (GER and N. Goldenfeld, PIs), the Christopher Foundation (GER), and the Illinois Sociogenomics Initiative (GER). Author contributions: B.M.J. and G.E.R. conceptualized the study and designed experiments; B.M.J. performed behavioral experiments; V.D.R., T.G., and T.J. developed methodology and software to collect and analyze data; B.M.J. and A.C-A. performed molecular work; B.M.J., B.E.R.R., T.J.C., S.B., S.S.H., and C.B. performed or aided in data analysis; M.M., S.S., S.C., and G.E.R. provided mentorship and project oversight throughout data collection, analysis, and interpretation. B.M.J. and G.E.R. drafted the initial manuscript; all authors contributed to editing and final writing of manuscript. Competing interests: The authors declare no competing interests. Data and materials availability: The raw sequence data reported in this paper have been deposited at the National Center for Biotechnology Information (NCBI) Sequence Read Archive, Accession PRJNA593999. Requests for materials should be addressed to B.M.J.

Competing interests

No competing interests declared.

References

Abadi M, Barham P, Chen J, Chen Z, Davis A, Dean J, Devin M, Ghemawat S, Irving G, Isard M, Kudlur M, Levenberg J, Monga R, Moore S, Murray DG, Steiner B, Tucker P, Vasudevan V, Warden P, Wicke M, Yu Y, Zheng X, Brain G, Osdi I, Barham P, Chen J, Chen Z, Davis A, Dean J, Devin M, Ghemawat S, Irving G, Isard M, Kudlur M, Levenberg J, Monga R, Moore S, Murray DG, Steiner B, Tucker P, Vasudevan V, Warden P, Wicke M, Yu Y, Zheng X. 2016. TensorFlow : A system for large-scale machine learning. *OSDI* **16**:265–283. doi:10.1126/science.aab4113.4

Adams J, Rothman ED, Kerr WE, Paulino ZL. 1977. Estimation of the number of sex alleles and queen matings from diploid male frequencies in a population of Apis mellifera. *Genetics* **86**:583–596.

Alaux C, Le Conte Y, Adams HA, Rodriguez-Zas S, Grozinger CM, Sinha S, Robinson GE. 2009. Regulation of brain gene expression in honey bees by brood pheromone. *Genes,*

895 *Brain Behav* **8**:309–319. doi:10.1111/j.1601-183X.2009.00480.x
896 Amdam G V, Page Jr RE, Tsuruda JM. 2008. Sensory response system of social behavior tied to
897 female reproductive traits. *PLoS One* **3**:e3397.
898 Araya CL, Kawli T, Kundaje A, Jiang L, Wu B, Vafeados D, Terrell R, Weissdepp P,
899 Gevirtzman L, Mace D, Niu W, Boyle AP, Xie D, Ma L, Murray JI, Reinke V, Waterston
900 RH, Snyder M. 2014. Regulatory analysis of the *C. elegans* genome with spatiotemporal
901 resolution. *Nature* **512**:400–405. doi:10.1038/nature16075
902 Bailey TL, Machanick P. 2012. Inferring direct DNA binding from ChIP-seq. *Nucleic Acids Res*
903 **40**:e128.
904 Barth RH, Lester LJ, Sroka P, Kessler T, Hearn R. 1975. Juvenile hormone promotes dominance
905 behavior and ovarian development in social wasps (*Polistes annularis*). *Experientia*
906 **31**:691–692. doi:10.1007/BF01944632
907 Benson G. 1999. Tandem repeats finder: A program to analyze DNA sequences. *Nucleic Acids*
908 *Res*. doi:10.1093/nar/27.2.573
909 Branstetter MG, Danforth BN, Pitts JP, Faircloth BC, Ward PS, Buffington ML, Gates MW,
910 Kula RR, Brady SG. 2017. Phylogenomic insights into the evolution of stinging wasps and
911 the origins of ants and bees. *Curr Biol* **27**:1019–1025. doi:10.1016/j.cub.2017.03.027
912 Buenrostro J, Giresi P, Zaba L, Chang H, Greenleaf W. 2013. Transposition of native chromatin
913 for fast and sensitive epigenomic profiling of open chromatin, DNA-binding proteins and
914 nucleosome position. *Nat Methods* **10**:1213–1218.
915 Buenrostro JD, Wu B, Chang HY, Greenleaf WJ. 2015. ATAC-seq: A Method for Assaying
916 Chromatin Accessibility Genome-Wide. *Curr Protoc Mol Biol* **109**:21.29.1-21.29.9.
917 Bukhari SA, Saul MC, James N, Bensky MK, Stein LR, Trapp R, Bell AM. 2019. Neurogenomic
918 insights into paternal care and its relation to territorial aggression. *Nat Commun* **10**:4437.
919 doi:10.1038/s41467-019-12212-7
920 Bukhari SA, Saul MC, Seward CH, Zhang H, Bensky M, James N, Zhao SD, Chandrasekaran S,
921 Stubbs L, Bell AM. 2017. Temporal dynamics of neurogenomic plasticity in response to
922 social interactions in male threespined sticklebacks. *PLoS Genet* **13**:e1006840.
923 doi:10.1371/journal.pgen.1006840
924 Chan YF, Marks ME, Jones FC, Villarreal G, Shapiro MD, Brady SD, Southwick AM, Absher
925 DM, Grimwood J, Schmutz J, Myers RM, Petrov D, Jónsson B, Schluter D, Bell MA,

926 Kingsley DM. 2010. Adaptive evolution of pelvic reduction in sticklebacks by recurrent
927 deletion of a pitxl enhancer. *Science* **327**:302–5. doi:10.1126/science.1182213
928 Chandrasekaran S. 2014. Predicting phenotype from genotype through reconstruction and
929 integrative modeling of metabolic and regulatory networksA Systems Theoretic Approach
930 to Systems and Synthetic Biology I: Models and System Characterizations. pp. 307–325.
931 doi:10.1007/978-94-017-9041-3_12
932 Chandrasekaran S, Ament SA, Eddy JA, Rodriguez-Zas SL, Schatz BR, Price ND, Robinson GE.
933 2011. Behavior-specific changes in transcriptional modules lead to distinct and predictable
934 neurogenomic states. *Proc Natl Acad Sci* **108**:18020.
935 Cnaani J, Schmid-Hempel R, Schmidt JO. 2002. Colony development, larval development and
936 worker reproduction in *Bombus impatiens* Cresson. *Insectes Soc* **49**:164–170.
937 doi:10.1007/s00040-002-8297-8
938 Crall JD, Gravish N, Mountcastle AM, Combes SA. 2015. BEEtag: A low-cost, image-based
939 tracking system for the study of animal behavior and locomotion. *PLoS One* **10**:e0136487.
940 doi:10.1371/journal.pone.0136487
941 Cummings ME, Larkins-Ford J, Reilly CRL, Wong RY, Ramsey M, Hofmann HA. 2008. Sexual
942 and social stimuli elicit rapid and contrasting genomic responses. *Proc R Soc B Biol Sci*
943 **275**:393–402. doi:10.1098/rspb.2007.1454
944 Dadant & Sons. 1975. Activities of queenless bees In: Dadant & Sons, editor. The Hive and the
945 Honey Bee. Carthage, Illinois: Journal Printing Company. pp. 245–247.
946 Dornhaus A. 2008. Specialization does not predict individual efficiency in an ant. *PLoS Biol*
947 **6**:2368–2375. doi:10.1371/journal.pbio.0060285
948 Dufour HD, Koshikawa S, Finet C. 2020. Temporal flexibility of gene regulatory network
949 underlies a novel wing pattern in flies. *Proc Natl Acad Sci U S A* **117**:11589–11596.
950 doi:10.1073/pnas.2002092117
951 Eden E, Navon R, Steinfeld I, Lipson D, Yakhini Z. 2009. GOrilla: A tool for discovery and
952 visualization of enriched GO terms in ranked gene lists. *BMC Bioinformatics* **10**:48.
953 doi:10.1186/1471-2105-10-48
954 Estoup A, Solignac M, Cornuet JM. 1994. Precise assessment of the number of patrilines and of
955 genetic relatedness in honeybee colonies. *Proc R Soc B Biol Sci* **258**:1–7.
956 doi:10.1098/rspb.1994.0133

957 Fine JD, Shpigler HY, Ray AM, Beach NJ, Sankey AL, Cash-Ahmed A, Huang ZY,
958 Astrauskaite I, Chao R, Zhao H, Robinson GE. 2018. Quantifying the effects of pollen
959 nutrition on honey bee queen egg laying with a new laboratory system. *PLoS One*
960 **13**:e0203444. doi:10.1371/journal.pone.0203444
961 Free JB. 1955. The behaviour of egg-laying workers of bumblebee colonies. *Br J Anim Behav*
962 **3**:147–153. doi:10.1016/S0950-5601(55)80053-6
963 Gadagkar R. 1997. The evolution of caste polymorphism in social insects genetic release
964 followed by diversifying evolution. *J Genet* **76**:167–179. doi:10.1007/BF02932215
965 Geffre AC, Gernat T, Harwood GP, Jones BM, Gysi DM, Hamilton AR, Bonning BC, Toth AL,
966 Robinson GE, Dolezal AG. 2020. Honey bee virus causes context-dependent changes in
967 host social behavior. *Proc Natl Acad Sci U S A*. doi:10.1073/pnas.2002268117
968 Gençer HV, Kahya Y. 2011. Are sperm traits of drones (*Apis mellifera* L.) from laying worker
969 colonies noteworthy? *J Apic Res* **50**:130–137. doi:10.3896/IBRA.1.50.2.04
970 Gernat T, Rao VD, Middendorf M, Dankowicz H, Goldenfeld N, Robinson GE. 2018.
971 Automated monitoring of behavior reveals bursty interaction patterns and rapid spreading
972 dynamics in honeybee social networks. *Proc Natl Acad Sci* **115**:1433–1438.
973 doi:10.1073/pnas.1713568115
974 Graham AM, Munday MD, Kaftanoglu O, Page RE, Amdam G V., Rueppell O. 2011. Support
975 for the reproductive ground plan hypothesis of social evolution and major QTL for ovary
976 traits of Africanized worker honey bees (*Apis mellifera* L.). *BMC Evol Biol* **11**:95.
977 doi:10.1186/1471-2148-11-95
978 Greenwald E, Segre E, Feinerman O. 2015. Ant trophallactic networks: simultaneous
979 measurement of interaction patterns and food dissemination. *Sci Rep* **5**:12496.
980 Grozinger CM, Fan Y, Hoover SER, Winston ML. 2007. Genome-wide analysis reveals
981 differences in brain gene expression patterns associated with caste and reproductive status
982 in honey bees (*Apis mellifera*). *Mol Ecol* **16**:4837–4848.
983 Hamilton AR, Shpigler H, Bloch G, Wheeler DE, Robinson GE. 2016. Endocrine Influences on
984 Insect Societies.Hormones, Brain and Behavior: Third Edition. doi:10.1016/B978-0-12-
985 803592-4.00037-7
986 Hamilton AR, Traniello IM, Ray AM, Caldwell AS, Wickline SA, Robinson GE. 2019. Division
987 of labor in honey bees is associated with transcriptional regulatory plasticity in the brain. *J*

988 *Exp Biol* **222**:jeb200196. doi:10.1242/jeb.200196
989 Harpur BA, Owayss AA, Lebon JMD, Zayed A, Alqarni AS, Molodtsova D, Kent CF. 2014.
990 Population genomics of the honey bee reveals strong signatures of positive selection on
991 worker traits. *Proc Natl Acad Sci* **111**:2614–2619.
992 Hess G. 1942. Über den einfluss der weisellosigkeit und des fruchtbarkeitsvitamins e auf die
993 ovarien der bienenarbeiterin. *Schweiz Bienen Ztg* **2**:33–110.
994 Holldobler B, Wilson EO. 1990. The Ants. Cambridge, MA: Belknap/Harvard Univ. Press.
995 Jeanson R, Clark RM, Holbrook CT, Bertram SM, Fewell JH, Kukuk PF. 2008. Division of
996 labour and socially induced changes in response thresholds in associations of solitary
997 halictine bees. *Anim Behav* **76**:593–602. doi:10.1016/j.anbehav.2008.04.007
998 Johnson WE, Li C, Rabinovic A. 2007. Adjusting batch effects in microarray expression data
999 using empirical Bayes methods. *Biostatistics* **8**:118–127. doi:10.1093/biostatistics/kxj037
1000 Jones BM, Kingwell CJ, Wcislo WT, Robinson GE. 2017. Caste-biased gene expression in a
1001 facultatively eusocial bee suggests a role for genetic accommodation in the evolution of
1002 eusociality. *Proc R Soc B Biol Sci* **284**:20162228.
1003 Kapheim KM, Jones BM, Pan H, Li C, Harpur BA, Kent CF, Zayed A, Ioannidis P, Waterhouse
1004 RM, Kingwell C, Stolle E, Avalos A, Zhang G, McMillan WO, Wcislo WT. 2020.
1005 Developmental plasticity shapes social traits and selection in a facultatively eusocial bee.
1006 *Proc Natl Acad Sci U S A* **117**:13615–13625. doi:10.1073/pnas.2000344117
1007 Kapheim KM, Pan H, Li C, Salzberg SL, Puiu D, Magoc T, Robertson HM, Hudson ME, Venkat
1008 A, Fischman BJ, Hernandez A, Yandell M, Ence D, Holt C, Yocum GD, Kemp WP, Bosch
1009 J, Waterhouse RM, Zdobnov EM, Stolle E, Kraus FB, Helbing S, Moritz RFA, Glastad KM,
1010 Hunt BG, Goodisman MAD, Hauser F, Grimmelikhuijzen CJP, Pinheiro DG, Nunes FMF,
1011 Soares MPM, Tanaka ÉD, Simões ZLP, Hartfelder K, Evans JD, Barribeau SM, Johnson
1012 RM, Massey JH, Southey BR, Hasselmann M, Hamacher D, Biewer M, Kent CF, Zayed A,
1013 Blatti C, Sinha S, Johnston JS, Hanrahan SJ, Kocher SD, Wang J, Robinson GE, Zhang G.
1014 2015. Genomic signatures of evolutionary transitions from solitary to group living. *Science*
1015 **348**:1139–1143.
1016 Lobo J, Kerr W. 1993. Estimation of the number of matings in *Apis mellifera*: extensions of the
1017 model and comparison of different estimates. *Ethol Ecol Evol* **5**:337–345.
1018 Mallarino R, Campàs O, Fritz JA, Burns KJ, Weeks OG, Brenner MP, Abzhanov A. 2012.

1019 Closely related bird species demonstrate flexibility between beak morphology and
1020 underlying developmental programs. *Proc Natl Acad Sci U S A* **109**:16222–16227.
1021 doi:10.1073/pnas.1206205109
1022 Mello C V, Vicario DS, Clayton DF. 1992. Song presentation induces gene expression in the
1023 songbird forebrain. *Proc Natl Acad Sci U S A* **89**:6818–6822. doi:10.1073/pnas.89.15.6818
1024 Mersch DP, Crespi A, Keller L. 2013. Tracking individuals shows spatial fidelity is a key
1025 regulator of ant social organization. *Science* **340**:1090. doi:10.1126/science.1234316
1026 Michener CD. 1974. The Social Behavior of the Bees: A Comparative Study. Cambridge, MA:
1027 Harvard University Press.
1028 Miller III DG, Ratnieks FLW. 2001. The timing of worker reproduction and breakdown of
1029 policing behaviour in queenless honey bee (*Apis mellifera* L.) societies. *Insectes Soc*
1030 **48**:178.
1031 Morse RA. 1990. Laying workers In: Morse RA, Flottum K, editors. The ABC & XYZ of Bee
1032 Culture. The A. I. Root Company. pp. 291–293.
1033 Mukherjee D, Ignatowska-Jankowska BM, Itskovits E, Gonzales BJ, Turm H, Izakson L, Haritan
1034 D, Bleistein N, Cohen C, Amit I, Shay T, Grueter B, Zaslaver A, Citri A. 2018. Salient
1035 experiences are represented by unique transcriptional signatures in the mouse brain. *Elife*
1036 **7**:e31220. doi:10.7554/eLife.31220
1037 Naeger NL, Peso M, Even N, Barron AB, Robinson GE. 2013. Altruistic behavior by egg-laying
1038 worker honeybees. *Curr Biol* **23**:1574–1578. doi:10.1016/j.cub.2013.06.045
1039 O'Donnell S. 1998. Reproductive caste determination in eusocial wasps (Hymenoptera:
1040 Vespidae). *Annu Rev Entomol* **43**:323–346. doi:10.1146/annurev.ento.43.1.323
1041 Oster GF, Wilson EO. 1979. Caste and Ecology in the Social Insects. Princeton: Princeton
1042 University Press. doi:10.1007/s00265-010-1009-x
1043 Page Jr RE, Erickson Jr EH. 1988. Reproduction by worker honey bees (Apis mellifera). *Behav*
1044 *Ecol Sociobiol* **23**:117–126. doi:10.1007/BF00299895
1045 Page Jr RE, Rueppell O, Amdam G V. 2012. Genetics of reproduction and regulation of honey
1046 bee (*Apis mellifera* L.) social behavior. *Annu Rev Genet* **46**:19–97.
1047 Page RE, Robinson GE. 1994. Reproductive competition in queenless honey bee colonies (*Apis*
1048 *mellifera* L.). *Behav Ecol Sociobiol* **35**:99–107. doi:10.1007/BF00171499
1049 Prud'homme B, Gompel N, Rokas A, Kassner VA, Williams TM, Yeh SD, True JR, Carroll SB.

1050 2006. Repeated morphological evolution through *cis*-regulatory changes in a pleiotropic
1051 gene. *Nature* **440**:1050–3. doi:10.1038/nature04597
1052 Ratnieks FLW, Foster KR, Wenseleers T. 2006. Conflict resolution in insect societies. *Annu Rev*
1053 *Entomol* **51**:581–608. doi:10.1146/annurev.ento.51.110104.151003
1054 Ratnieks FLW, Wenseleers T. 2008. Altruism in insect societies and beyond: voluntary or
1055 enforced? *Trends Ecol Evol* **23**:45–52. doi:10.1016/j.tree.2007.09.013
1056 Reed RD, Papa R, Martin A, Hines HM, Counterman BA, Pardo-Diaz C, Jiggins CD,
1057 Chamberlain NL, Kronforst MR, Chen R, Halder G, Nijhout HF, McMillan WO. 2011.
1058 optix drives the repeated convergent evolution of butterfly wing pattern mimicry. *Science*
1059 **333**:1137.
1060 Rittschof CC, Bukhari SA, Sloofman LG, Troy JM, Caetano-Anollés D, Cash-Ahmed A, Kent
1061 M, Lu X, Sanogo YO, Weisner PA, Zhang H, Bell AM, Ma J, Sinha S, Robinson GE,
1062 Stubbs L. 2014. Neuromolecular responses to social challenge: Common mechanisms
1063 across mouse, stickleback fish, and honey bee. *Proc Natl Acad Sci* **111**:17929–17934.
1064 Robinson GE. 1992. Regulation of division of labor in insect societies. *Annu Rev Entomol*
1065 **37**:637–665.
1066 Robinson GE, Page RE, Fondrk MK. 1990. Intracolonial behavioral variation in worker
1067 oviposition, oophagy, and larval care in queenless honey bee colonies. *Behav Ecol*
1068 *Sociobiol* **26**:315–323. doi:10.1007/BF00171096
1069 Robinson GE, Strambi C, Strambi A, Huang ZY. 1992. Reproduction in worker honey bees is
1070 associated with low juvenile hormone titers and rates of biosynthesis. *Gen Comp*
1071 *Endocrinol* **87**:471–480. doi:10.1016/0016-6480(92)90055-O
1072 Sakagami SF. 1954. Occurrence of an aggressive behaviour in queenless hives, with
1073 considerations on the social organization of honeybee. *Insectes Soc* **1**:331–343.
1074 doi:10.1007/BF02329618
1075 Saul MC, Seward CH, Troy JM, Zhang H, Sloofman LG, Lu X, Weisner PA, Caetano-Anolles
1076 D, Sun H, Zhao SD, Chandrasekaran S, Sinha S, Stubbs L. 2017. Transcriptional regulatory
1077 dynamics drive coordinated metabolic and neural response to social challenge in mice.
1078 *Genome Res* **27**:959–972. doi:10.1101/gr.214221.116
1079 Schindelin J, Arganda-Carreras I, Frise E, Kaynig V, Longair M, Pietzsch T, Preibisch S,
1080 Rueden C, Saalfeld S, Schmid B, Tinevez JY, White DJ, Hartenstein V, Eliceiri K,

1081 Tomancak P, Cardona A. 2012. Fiji: An open-source platform for biological-image
1082 analysis. *Nat Methods* **9**:676. doi:10.1038/nmeth.2019
1083 Schulz DJ, Robinson GE. 1999. Biogenic amines and division of labor in honey bee colonies:
1084 Behaviorally related changes in the antennal lobes and age-related changes in the mushroom
1085 bodies. *J Comp Physiol A* **184**:481–488. doi:10.1007/s003590050348
1086 Seeley TD. 2009. The Wisdom of the Hive: the social physiology of honey bee colonies,
1087 Proceedings of the Royal Society B: Biological Sciences. doi:10.1098/rspb.2010.0491
1088 Shpigler HY, Saul MC, Murdoch EE, Cash-Ahmed AC, Seward CH, Sloofman L,
1089 Chandrasekaran S, Sinha S, Stubbs LJ, Robinson GE. 2017. Behavioral, transcriptomic and
1090 epigenetic responses to social challenge in honey bees. *Genes, Brain Behav* **16**:579–591.
1091 doi:10.1111/gbb.12379
1092 Simola DF, Graham RJ, Brady CM, Enzmann BL, Desplan C, Ray A, Zwiebel LJ, Bonasio R,
1093 Reinberg D, Liebig J, Berger SL. 2015. Epigenetic (re)programming of caste-specific
1094 behavior in the ant *Camponotus floridanus*. *Science* **351**:aac6633.
1095 Sinha S, Jones BM, Traniello IM, Bukhari SA, Halfon MS, Hofmann HA, Huang S, Katz PS,
1096 Keagy J, Lynch VJ, Sokolowski MB, Stubbs LJ, Tabe-Bordbar S, Wolfner MF, Robinson
1097 GE. 2020. Behavior-related gene regulatory networks: A new level of organization in the
1098 brain. *Proc Natl Acad Sci U S A*. doi:10.1073/pnas.1921625117
1099 Sinha S, Ling X, Whitfield CW, Zhai C, Robinson GE. 2006. Genome scan for *cis*-regulatory
1100 DNA motifs associated with social behavior in honey bees. *Proc Natl Acad Sci U S A*
1101 **103**:16352–16357. doi:10.1073/pnas.0607448103
1102 Sinha S, van Nimwegen E, Siggia ED. 2003. A probabilistic method to detect regulatory
1103 modules. *Bioinformatics* **19 Suppl 1**:i292-301. doi:10.1093/bioinformatics/btg1040
1104 Storey JD, Bass AJ, Dabney A, Robinson D. 2019. qvalue: Q-value estimation for false
1105 discovery rate control. R package version 2.14.1.
1106 Toth AL, Várala K, Henshaw MT, Rodriguez-Zas SL, Hudson ME, Robinson GE. 2010. Brain
1107 transcriptomic analysis in paper wasps identifies genes associated with behaviour across
1108 social insect lineages. *Proc R Soc B Biol Sci* **277**:2139–2148. doi:10.1098/rspb.2010.0090
1109 Trumbo ST, Robinson GE. 1997. Learning and task interference by corpse-removal specialists in
1110 honey bee colonies. *Ethology* **103**:966–975. doi:10.1111/j.1439-0310.1997.tb00138.x
1111 Turillazzi S, West-Eberhard M. 1996. Natural History and Evolution of Paper-Wasps. Oxford:

1112 Oxford University Press.
1113 Velthuis HHW. 1970. Ovarian development in *Apis mellifera* worker bees. *Entomol Exp Appl*
1114 **13**:377.
1115 Velthuis HHW, Duchateau MJ. 2011. Ovarian development and egg laying in workers of
1116 *Bombus terrestris*. *Entomol Exp Appl* **51**:199–213.
1117 Wario F, Wild B, Couvillon MJ, Rojas R, Landgraf T. 2015. Automatic methods for long-term
1118 tracking and the detection and decoding of communication dances in honeybees. *Front Ecol*
1119 *Evol* **3**:103. doi:10.3389/fevo.2015.00103
1120 Wenseleers T, Ratnieks FLW. 2006. Enforced altruism in insect societies. *Nature* **444**:50.
1121 doi:10.1038/444050a
1122 Werner T, Koshikawa S, Williams TM, Carroll SB. 2010. Generation of a novel wing colour
1123 pattern by the Wingless morphogen. *Nature* **464**:1143–1148. doi:10.1038/nature08896
1124 West-Eberhard MJ. 1987. Flexible strategy and social evolution, Animal societies: theories and
1125 facts. Tokyo: Japan Scientific Societies Press.
1126 Wheeler DE. 1986. Developmental and physiological determinants of caste in social
1127 Hymenoptera: Evolutionary implications. *Am Nat* **128**:13–34.
1128 Whitfield CW, Cziko AM, Robinson GE. 2003. Gene expression profiles in the brain predict
1129 behavior in individual honey bees. *Science* **302**:296–299. doi:10.1126/science.1086807
1130 Whitney O, Pfenning AR, Howard JT, Blatti CA, Liu F, Ward JM, Wang R, Audet JN, Kellis M,
1131 Mukherjee S, Sinha S, Hartemink AJ, West AE, Jarvis ED. 2014. Core and region-enriched
1132 networks of behaviorally regulated genes and the singing genome. *Science* **346**:1256780.
1133 doi:10.1126/science.1256780
1134 Wilson EO. 1980. Caste and division of labor in leaf-cutter ants (Hymenoptera: Formicidae:
1135 *Atta*). *Behav Ecol Sociobiol* **7**:157–165. doi:10.1007/BF00299521
1136 Wilson EO. 1971. The insect societies. Cambridge: Harvard University Press.
1137 Woodard SH, Fischman BJ, Venkat A, Hudson ME, Varala K, Cameron SA, Clark AG,
1138 Robinson GE. 2011. Genes involved in convergent evolution of eusociality in bees. *Proc*
1139 *Natl Acad Sci* **108**:7472–7477. doi:10.1073/pnas.1103457108
1140 Zayed A, Robinson GE. 2012. Understanding the relationship between brain gene expression and
1141 social behavior: Lessons from the honey bee. *Annu Rev Genet* **46**:591–615.
1142 Zhu LJ, Christensen RG, Kazemian M, Hull CJ, Enuameh MS, Basciotta MD, Brasefield JA,

Zhu C, Asriyan Y, Lapointe DS, Sinha S, Wolfe SA, Brodsky MH. 2011. FlyFactorSurvey: A database of *Drosophila* transcription factor binding specificities determined using the bacterial one-hybrid system. *Nucleic Acids Res*. doi:10.1093/nar/gkq858

Supplemental Figures

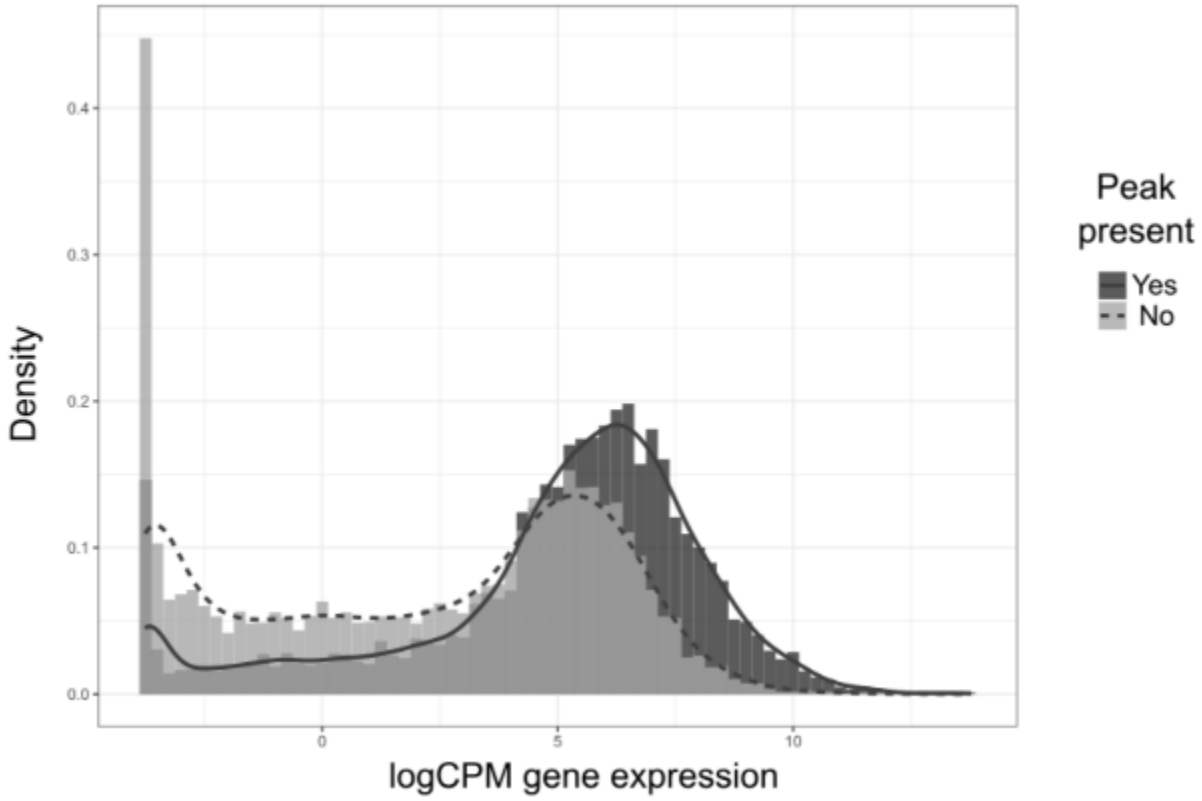

Fig. S1. Histogram (bars) and density (lines) of normalized (logCPM) gene expression for genes with (dark gray) and without (light gray) nearby peaks of chromatin accessibility. Distributions are significantly different ($p<0.0001$, Kolmogorov-Smirnov test).

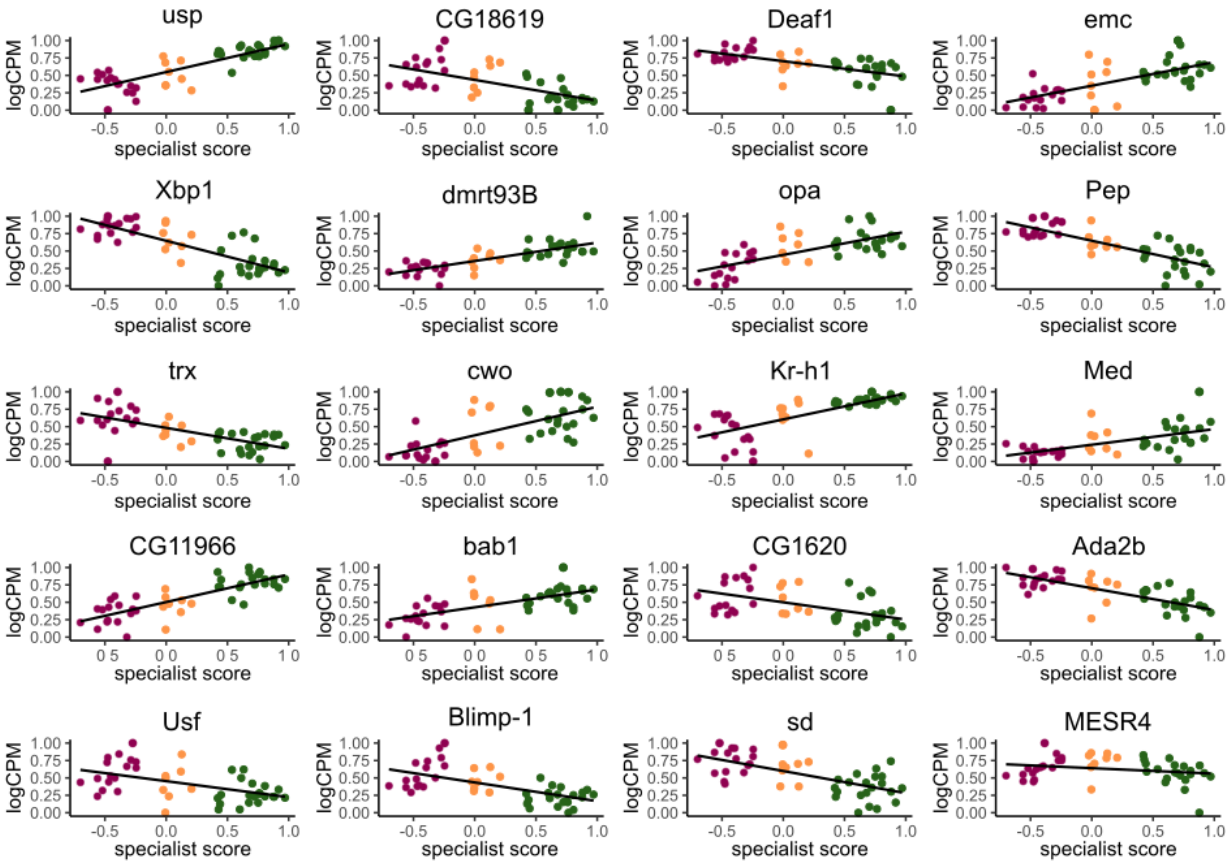

Fig. S2. Normalized expression (logCPM, scaled to a maximum of 1 to allow for comparison across TFs) of the top 20 most informative TFs for class prediction analysis plotted against individual specialist score. Points are colored by behavioral group (Layer: purple, Generalist: orange, Forager: green). Although some of the top predictors individually show weak correlation with specialist score, the random forest machine learning algorithm combined multiple weak predictors together in a single model to accurately classify the three behavioral groups, suggesting the TFs act combinatorially to influence behavior.

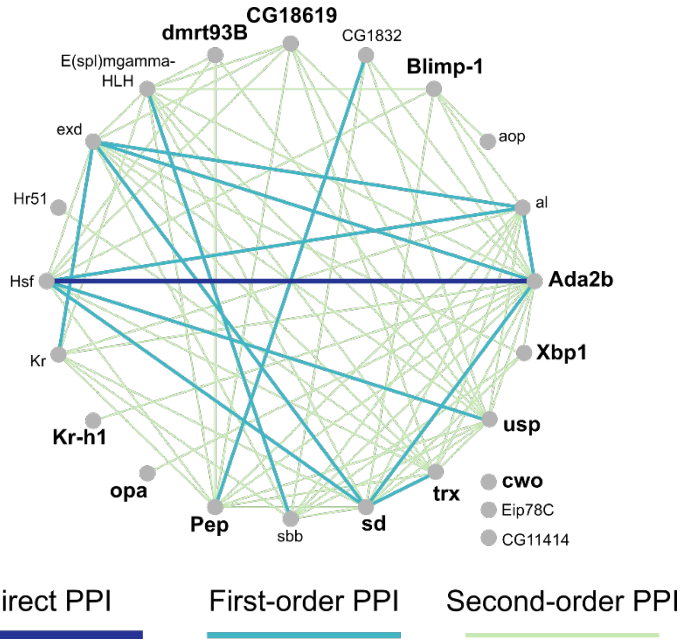

Fig. S3. Network of 23 TFs with module expression significantly correlated with 9 behavioral and physiological metrics (see File S2) measured across individuals. Edges indicate known interactions based on MIST database for Drosophila melanogaster. First-order PPI indicates one intermediate protein between linked nodes, while second-order PPI indicates two intermediate proteins. PPI = protein-protein interaction.

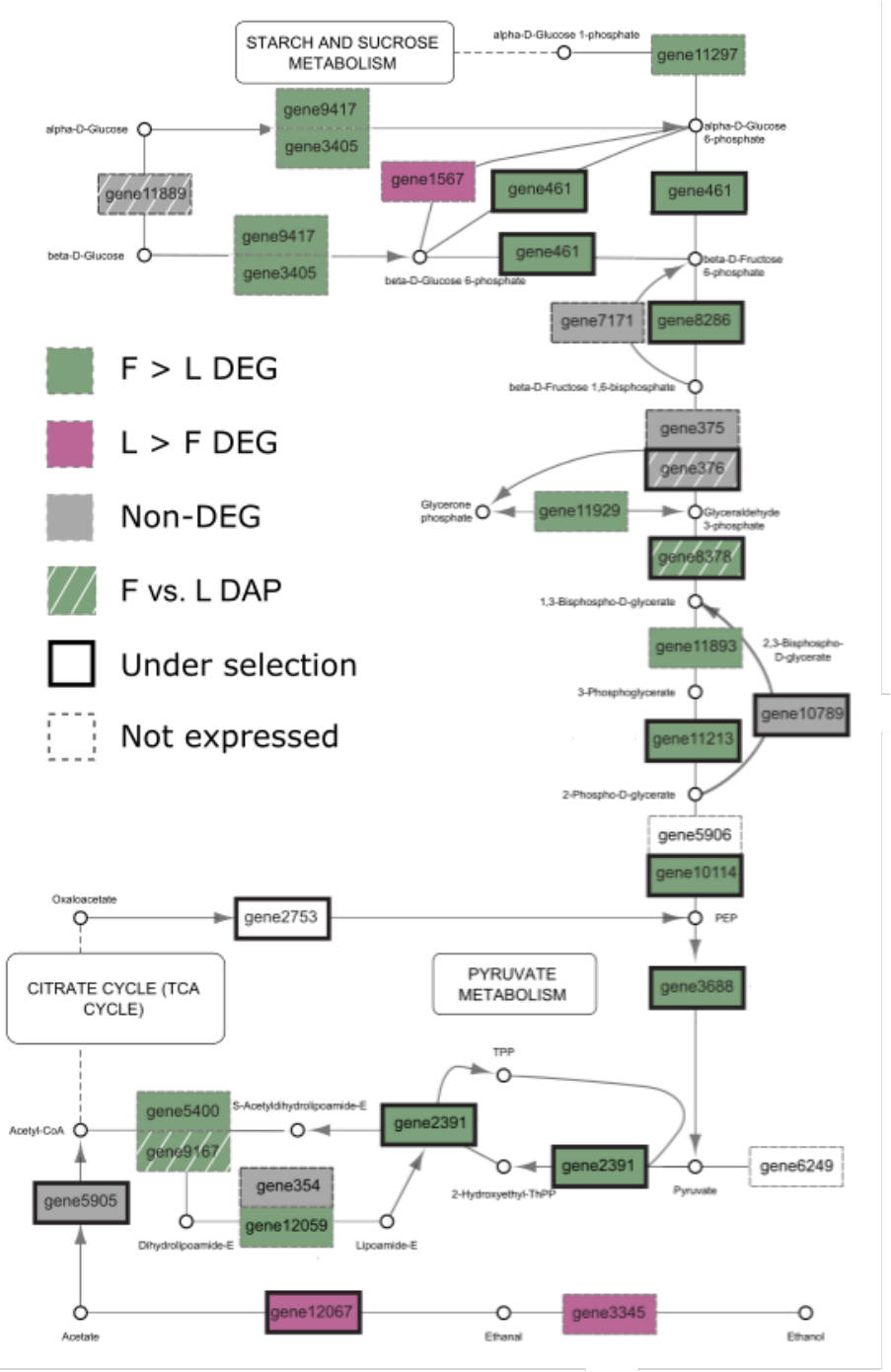

Fig. S4. Annotated honey bee genes in the glycolysis/gluconeogenesis KEGG pathway (Kyoto Encyclopedia of Genes and Genomes, http://www.genome.jp/kegg/). Genes are colored to indicate whether they are differentially expressed (DEG) between foragers (F) and layers (L), and hashed if they have a nearby differentially accessible peak (DAP). Thick borders indicate genes which were found to be under selection in at least one of three studies of selection in bees (Harpur et al., 2014; Kapheim et al., 2015; Woodard et al., 2011). "Not expressed" genes refer to those not expressed above the minimum threshold in the F vs. L dataset, while non-DEG genes were expressed but not differentially expressed in F vs. L at an FDR-corrected $p<0.05$.

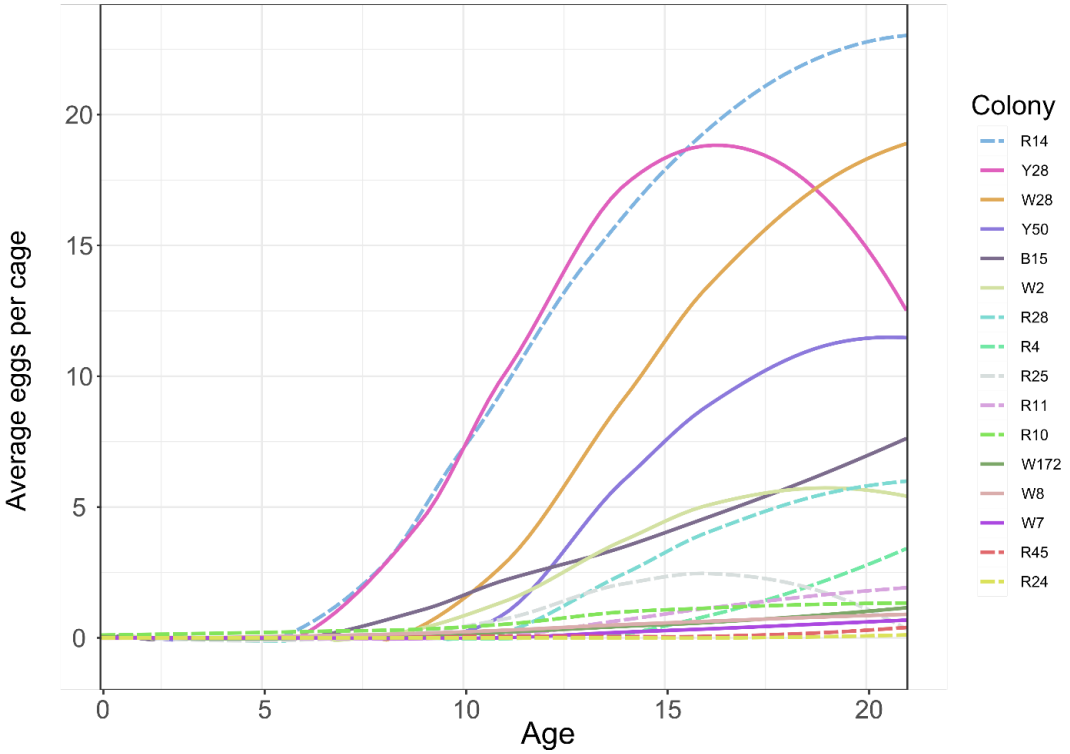

Fig. S5. Smoothed average egg counts for laying workers in laboratory cages. Solid lines indicate bees from source colonies headed by a naturally-mated queen, while dashed lines indicate bees from source colonies headed by queens instrumentally inseminated with semen from a single drone (SDI).

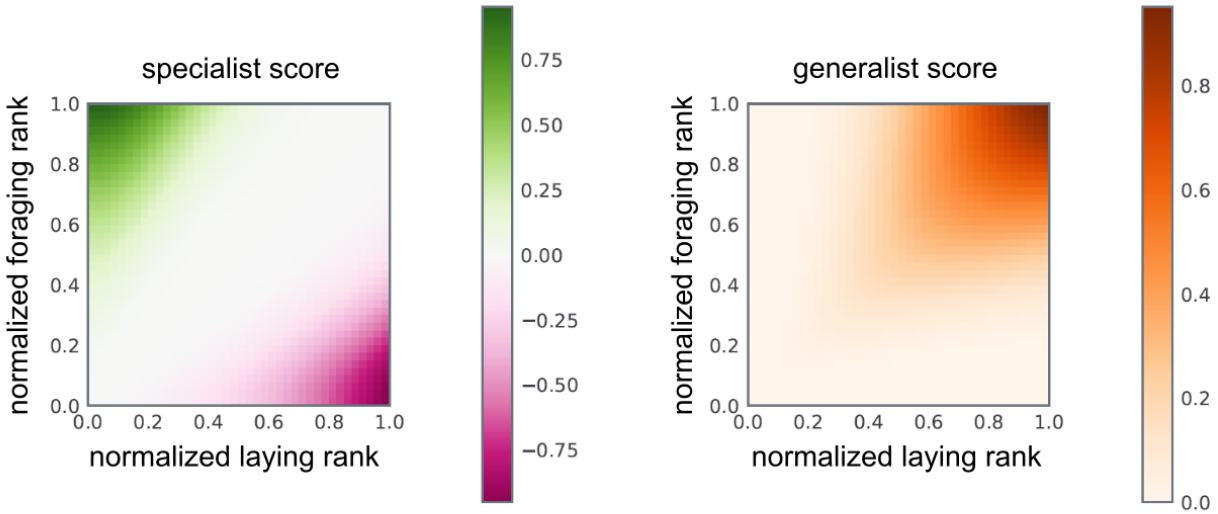

$$\text{specialist score} = \sin\left(\theta - \frac{\pi}{4}\right)\rho^4 \cos^4 2\theta \qquad \text{generalist score} = \frac{1}{2}\rho^2 \sin^4 2\theta$$

Fig. S6. Formulae and color-space mapping for specialist (left) and generalist (right) behavioral scores.

1185 **Supplemental Files**

1186 **File S1:** Daily egg-laying counts, foraging counts, specialist scores, and generalist scores for
1187 individual bees

1188 **File S2:** Detailed behavioral and physiological information for sequenced bees

1189 **File S3:** Differentially expressed genes (DEGs) and Gene Ontology (GO) enrichment of DEGs
1190 for each pairwise comparison of specialists and generalists

1191 **File S4:** Differentially accessible peaks (DAPs) and Gene Ontology (GO) enrichment of DAPs
1192 for each pairwise comparison of specialists and generalists

1193 **File S5:** Lists of genes with upper and lower 5% of PC loadings for gene expression and Gene
1194 Ontology (GO) enrichment results

1195 **File S6:** Lists of genes with upper and lower 5% of PC loadings for chromatin accessibility and
1196 Gene Ontology (GO) enrichment results

1197 **File S7:** TF motif enrichment of DAPs and DEGs

1198 **File S8:** Predicted gene regulatory network (GRN), GRN module correlations with behavior and
1199 physiological measurements, and importance scores of TFs from class prediction analysis

1200 **File S9:** Overlaps and statistics for comparative gene expression datasets

1201 **File S10:** Details of experimental setup for recorded colonies